

IEEE RADAR CONFERENCE 2010
May 10-14, 2010 Washington DC, USA

Tutorial T-18: SAR Signal and Image Processing for ISR Applications

Uttam K. Majumder, AFRL Sensors Directorate
Mehrdad Soumekh, Soumekh Consulting



References

1. Soumekh, M., *Synthetic Aperture Radar Signal Processing with MATLAB Algorithms*, Wiley, 1999.
2. Barnes, C., "SAR Image Formation Processing Course Notes," Georgia Tech Research Institute.
3. Jakowatz, C., et.al., *Spotlight-Mode SAR: A Signal Processing Approach*, Kluwer Academic Publishers, Boston, 1996.
4. XPatch User Manual. SAIC-DEMACO, Champaign, Illinois.
5. Backues, M., Majumder, U. "Embedded Gotcha Radar Exploitation with GPU-Based Backprojection Image Formation," AFRL/RYS In-house Research, 2009.
6. Steed, J., Majumder, U., Lundgren, W., Backues, M., "Implementing SAR Image Processing Using Backprojection on the Cell Broadband Engine," Proceedings of IEEE Radar Conference 2008, Rome, Italy.
7. Backues, M., Majumder, U., Casteel, C., Minardi, M., Gorham, L., Scarborough, S., York, D., "SAR Backprojection on a Sony Playstation 3," In Algorithms for Synthetic Aperture Radar Imagery XV, Edmund G. Zelnio, Frederick D. Garber, Editors, Proceedings of SPIE Vol. 6970, 2008.
8. Minardi, M., "Computational Efficiencies of Back Projection vs. Digital Spotighting Followed by Back Projection," AFRL/RYS In-house Research, 2008.

**This Document has been approved for public release by
88 ABW/PA on 04-MAY-10 as Document Number 88 ABW-10-2412.**

Course Outline

0. Conventional linear SAR data collection and processing
1. Advantages of *nonlinear* multi-channel, multi-polarization SAR data (30 minutes)
2. Video SAR processing (60 minutes)
3. Coherent and non-coherent change detection (45 minutes)
4. Multiple moving target detection and tracking (75 minutes)
5. Multi-touch screen interface for SAR data visualization (15 minutes)
6. Summary

0. Conventional Linear SAR Data Collection and Processing

SAR Data Collection Geometry

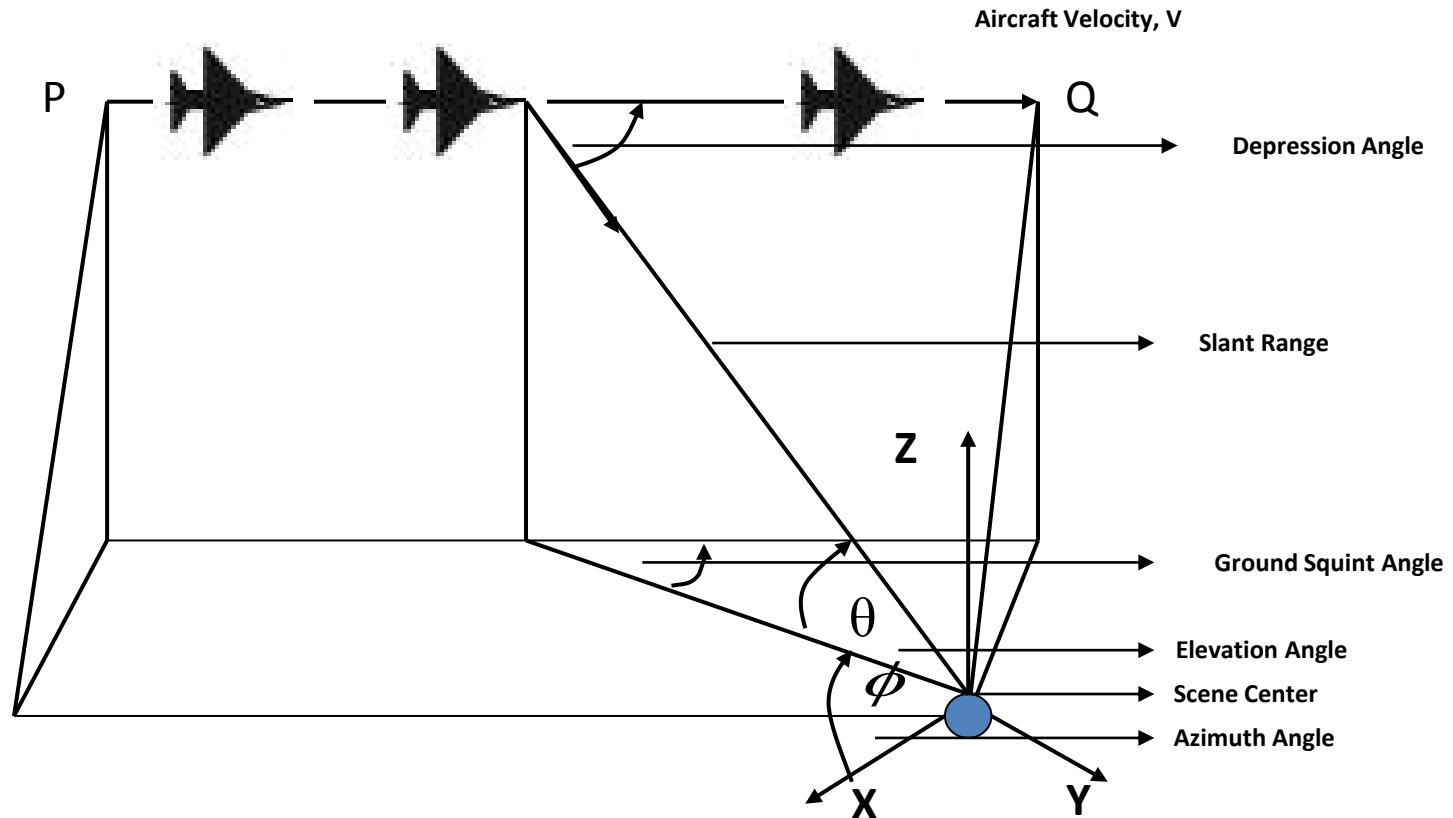


Figure : SAR Data Collection [4]

SAR Data Collection Modalities: Stripmap SAR

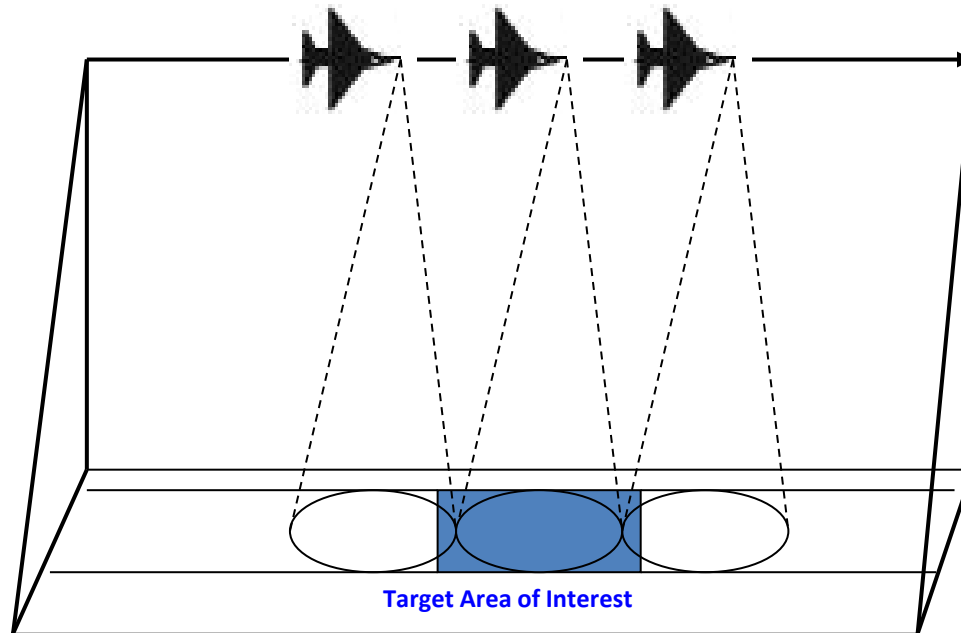


Figure : Stripmap SAR data collection [1,2]

SAR Data Collection Modalities: Spotlight SAR

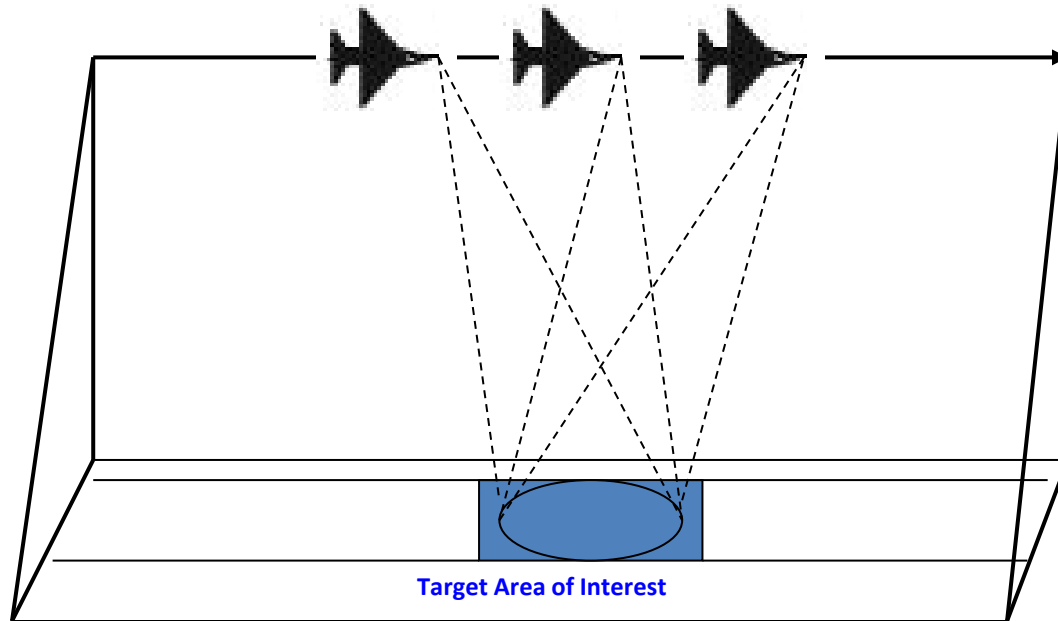


Figure : Spotlight SAR data collection [1,2]

SAR Data Collection Modalities: Interferometric SAR (IFSAR)

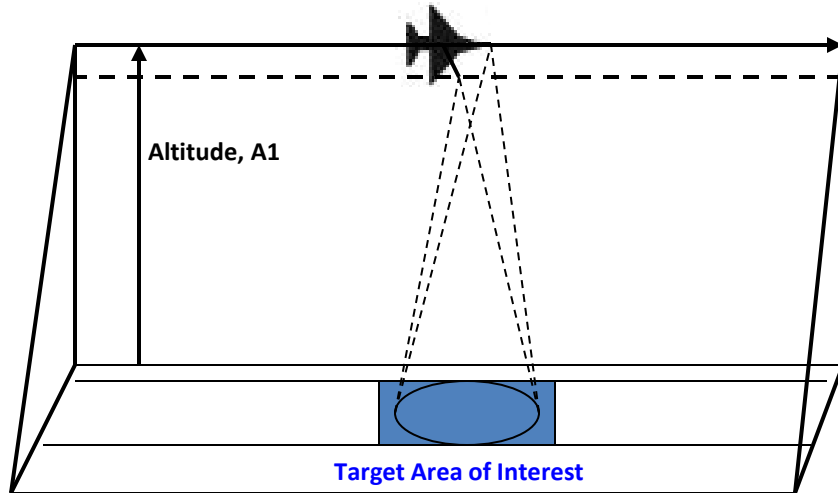


Figure : Single-pass IFSAR data collection [3]

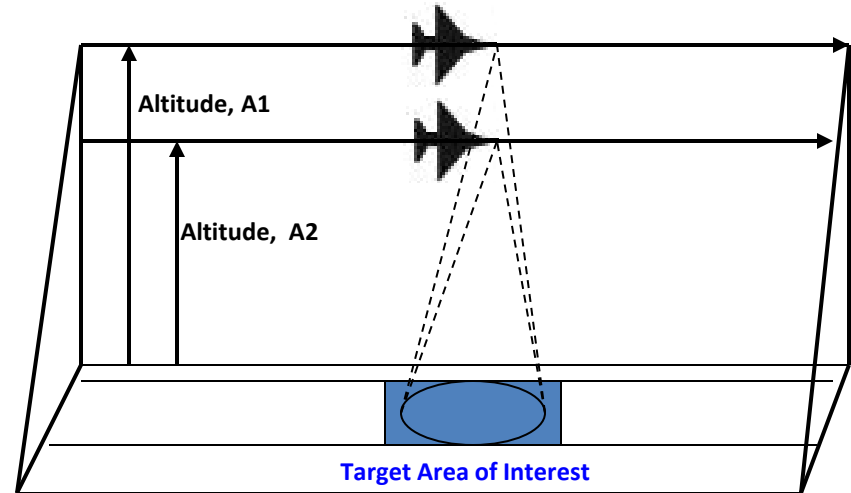


Figure : Two-pass IFSAR data collection [3]

Issues with Linear SAR Data Collection and Conventional Processing

- Most operational SAR platforms utilize a *linear flight* path to interrogate an imaging scene
- Such data acquisition provides limited Doppler and aspect angle information for target classification and perhaps identification and moving target detection and tracking
- The capability of these SAR systems is further limited due to the fact that the approximation-based Polar Format Processing (PFP) algorithm is used to analyze and/or image from the acquired data
- The PFP method results in erroneous phase information and undesirable spatial warping that are particularly problematic in SAR-MTI, motion tracking and moving target imaging

1. Advantages of Nonlinear Multi-Channel, Multi- Polarization SAR Data

SAR Data Collection Modalities: Circular SAR (CSAR)

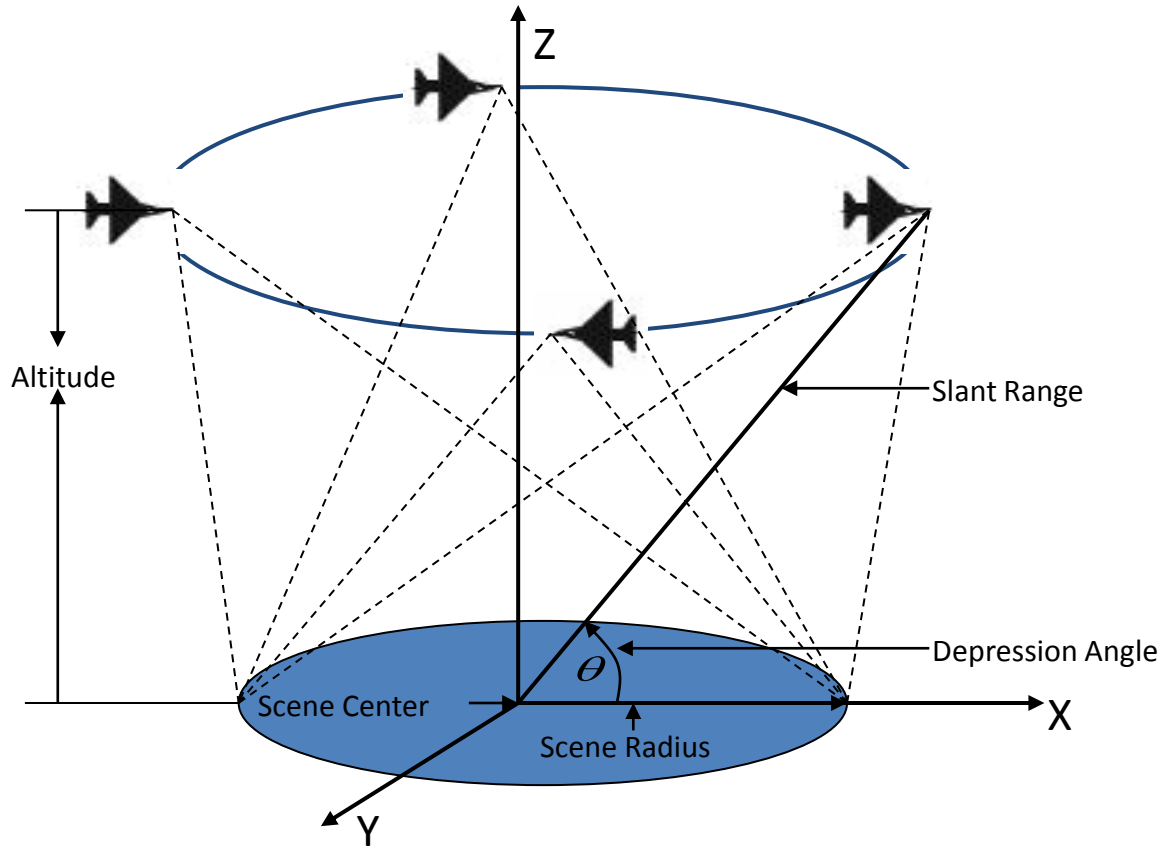


Figure : Circular SAR data collection

Nonlinear or Circular SAR

- A more effective approach for SAR target classification and SAR-MTI problems is to interrogate a scene with a platform that moves along a *circular path (CSAR, Circular SAR)* [2]-[3]
- CSAR data acquisition strategy enables the user to *see a target at various aspect angles; this increases the probability of detecting a weak target such as a human being (a dismount)* [1]

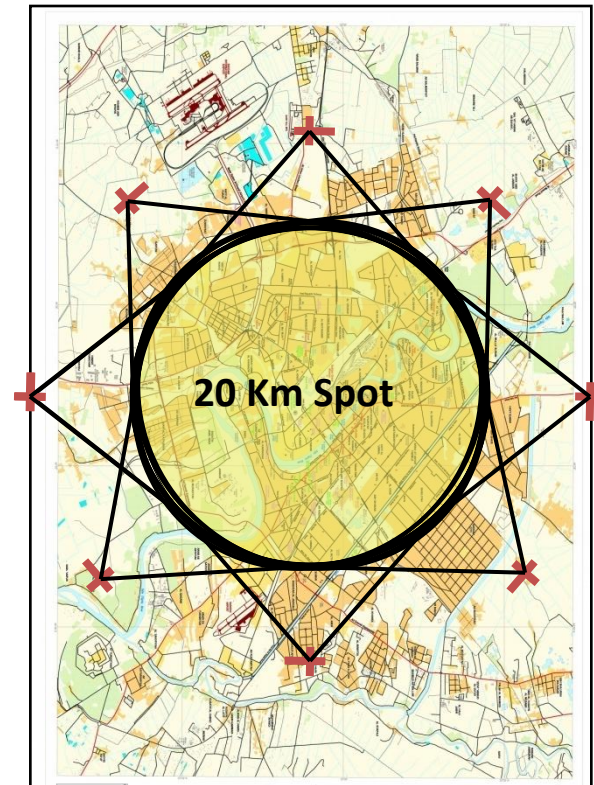
- Furthermore, the single or dual channel SAR-MTI methods are most effective when the target motion path is perpendicular to the SAR platform motion path while the algorithms fail when the target motion path is parallel to the SAR platform motion path. Thus, a SAR platform on a circular trajectory (CSAR) has the ability to detect moving targets within a wide range of motion paths.
- Multi-Polarization SAR data allows Polarimetric Video SAR processing and Polarimetric Change Detection

CSAR Allows Persistent Staring ISR

Persistence – Temporal Constancy / Angular Diversity

- Continuous circular orbit
 - for hours or days
- Single mode observing a single wide area
 - No observation gaps – detect angular and temporal transients
 - Minimizes sensor resource management
 - Enables Tracking in dense Urban Environments
- Record and rapidly transmit raw data
- Use high-performance computing to exploit information rapidly, and to perform forensic analysis.

Continuous Scan of Area of Interest



Persistent SAR Data Products



VIDEO SAR

1600 processors

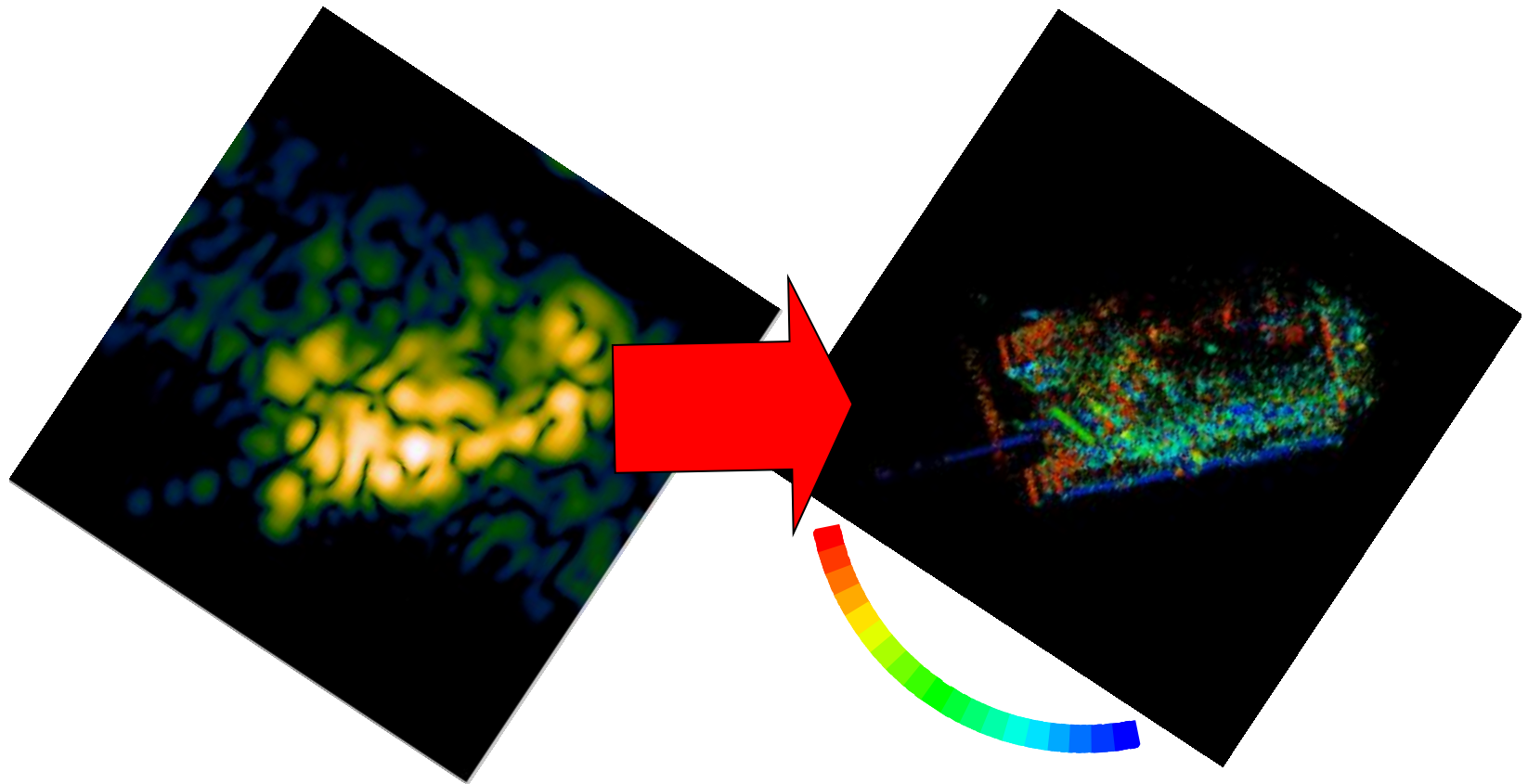
Real-time

BACKPROJECTION TO DEM

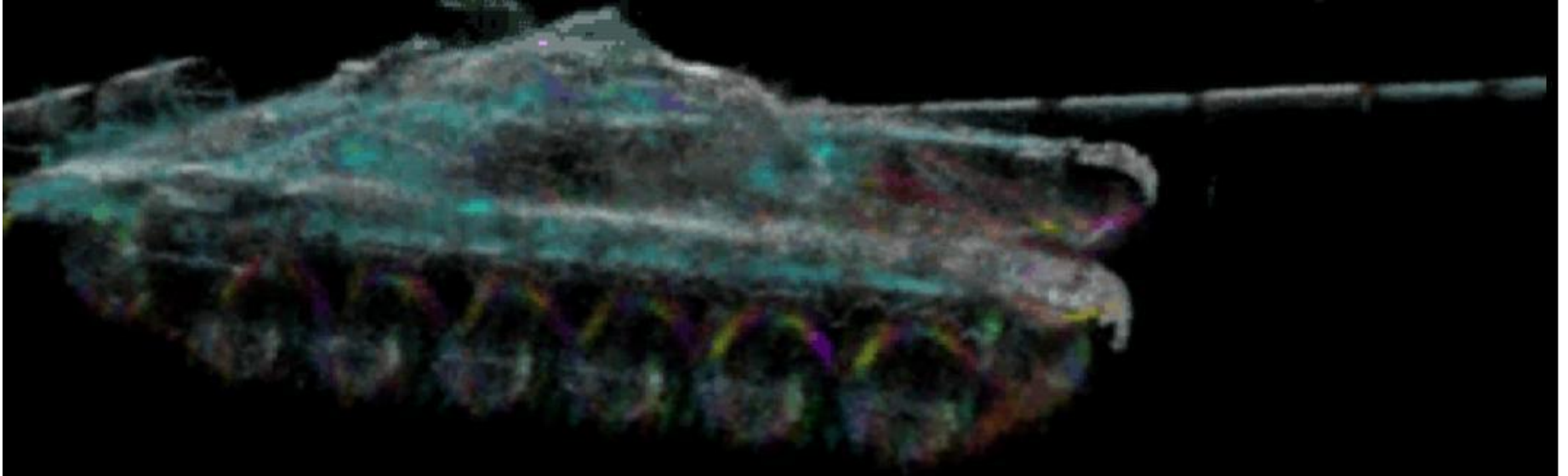
- **Computationally intensive**
- **“Embarrassingly parallel”**

AFRL Public Release: WPAFB-08-1102

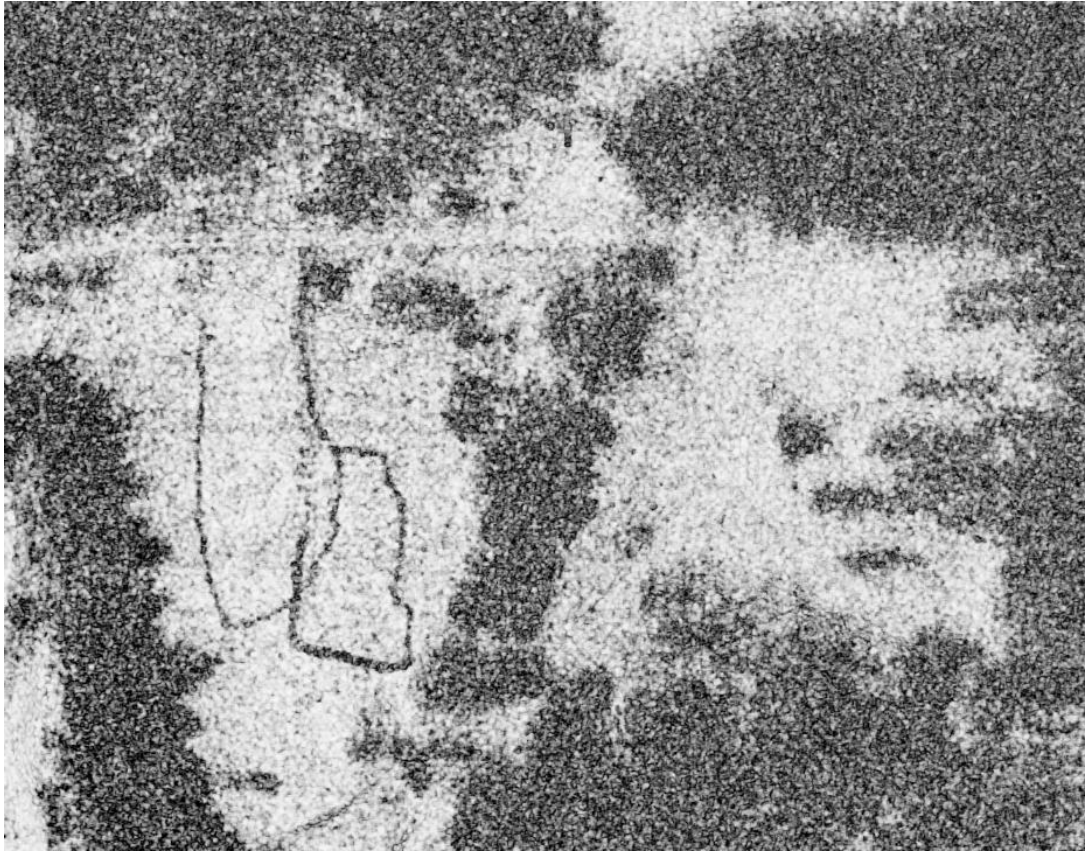
High Res Imagery from Wide Apertures



Theoretical Limit for SAR Imagery?



Video CCD



WPAFB-08-1102

2. Video SAR Processing

Video SAR Imaging Algorithms

- Most commonly used Video SAR Processing algorithms are:
 1. Polar Format Processing
 2. Backprojection (Time Domain Correlation, TDC)
 3. Range Migration (RMA)
 4. Wavefront
- RMA and Wavefront are based on the same Fourier-based principles; however, Wavefront is capable of ***3D spatially-varying motion compensation*** using INS data that are also used by Backprojection
- Backprojection is the preferred method due to its simplicity (30 lines of code versus more than 3000 lines of code for Wavefront)

Real-time Video SAR generation Using a Supercomputer

- Following sections will provide real-time video SAR Processing using a supercomputer called “DESCH”
 1. Supercomputer DESCH
 2. Vision of Wide area Video SAR Processing
 3. Discussion on overall technical approach
 4. Two-stage Backprojection Algorithm

DESCH



- 22 .9 TFlop/second, Quad Core Intel Nehalem Processor
- 2048 Cores, 2.8 GHz
- 3 TB RAM (1066 MHz DDR3)
- 87 TB Fast Data Storage (Lustre File System)
- 4x DDR (16 Giga Bits Per Second)
- 308th on Top 500 Supercomputer List (June 2009)

Public Release: Document Number 88 ABW-10-2208

Vision for Wide area Video SAR Processing

- Provide real-time 24/7, all weather, persistent staring surveillance capability and exploitation products
 - Video SAR, Change Detection, Ground Moving Target Indication (GMTI), Super resolution imagery
- A very large ground area coverage
- Real-time On-board / ground processing

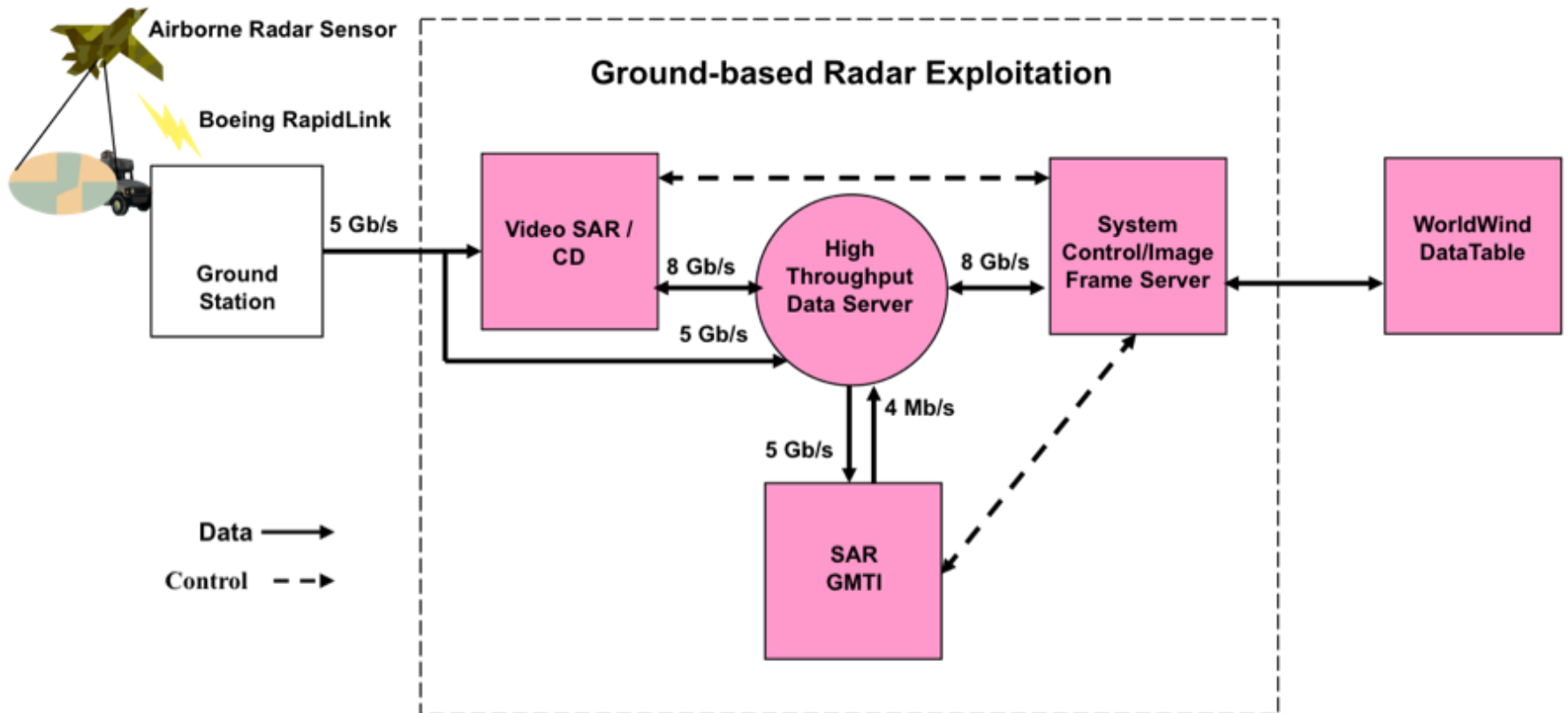
Discussion on overall technical approach

- To meet users need provide capabilities with increasing ground coverage as HPC technology improves over time:
 - Small area Video SAR @ 1 frame/sec.
 - Large area Video SAR @ 1 frame/sec.
 - Very large area Video SAR @ 1 frame/sec.
- Small area Video SAR production, 1 frame/s
 - Requires about 58 Tflop/s (1/3 m resolution)
 - Requires about 132 Tflop/s (1/4 m resolution)

Discussion on overall technical approach

- Supercomputer Desch provides 22.9 Tflop/s (peak)
- Algorithmic innovation reduced complexity:
 - Gold Standard SAR Image Formation has $O(N^3)$ complexity
 - AFRL/RVAS developed $O(N^{2.5})$ Video SAR algorithm, known as 2-stage Backprojection (BP)
- The 2-stage BP reduces
 - Floating point operation count for one 20000x20000 pixel image from 132 Tflop to 2.6 Tflop
 - Demands for interprocessor communication

Real-time Video SAR Processing Block Diagram



Two-Stage Backprojection

- Computational Efficiencies are achieved by Digital Spotlighting Followed by Back Projection (DSBP)
- Assume we want to form a SAR image with $N \times N$ pixels. Assume that the input data is of the form of N compressed range profiles with each profile having N samples
- An individual back projection operation is defined as taking a single range profile and back projecting it to a single pixel. To form a complete back projected image we need to back project the N range profiles to N^2 pixels. That gives us N^3 individual back projection operations. If an individual back projection operation needs p floating point operations then we have pN^3 floating point operations to make a complete $N \times N$ image.
- Now break up the image into an $m \times m$ grid of subimages. Each of m^2 subimages has $(N/m)^2$ pixels.

Source: Minardi, M., "Computational Efficiencies of Back Projection vs. Digital Spotlighting Followed by Back Projection," **AFRL/RVAS In-house Research**, 2008.

Two-Stage BP

- The proposed two-stage algorithm will be to do digital spotlighting to create a lower PRF phase history input to each sub-image and then do BP for the image.

- The DSBP algorithm is a little more complicated of course.

The Digital Spotlight (DS) stage consists of 3 steps:

- Step 1: cut out the proper subrange of the range profile. The subrange will contain the N/m range bins needed for the current subpatch of the scene.

I will assume that the flops needed to do this can be neglected.

- Step 2: re-center the range profile to the local scene center. This could be implemented with a FIR filter that is r taps long. The filter will resample the data so the center range bin in the profile is *exactly* at the range to local scene center for that pulse. Each tap in the FIR filter will have an additional phase adjustment built into it so that any return from local scene center has a constant phase for all pulses (i.e. the return would show up with zero Doppler in a range-Doppler map of the data).

- Step 3) Lowpass filter and decimate the data across pulses (AKA slow time). This step is the key to the computational savings of the two-stage DSBP algorithm. Note that step 2 has conditioned the data so that returns from the local scene center are at zero Hz Doppler.

Two-Stage BP cont..

Further note that we are now only concerned with a smaller group of pixels clustered around the new local scene center. The subpatch has $1/m$ of the cross range extent of the full scene. Therefore, we can take the data from any given range bin and lowpass filter it across the N pulses and be guaranteed that we have preserved all of the returns from scatterers in the sub-patch of ground we are currently concerned with.

Computation Costs for 2-stage BP

Step 2 will require:

8 flops to do a complex multiply,
 r complex multiplies to create a resampled rangebin,
 N/m rangebins to create a recentered range profile,
 N recentered range profiles and
 m^2 local scenes.

Multiply them all together to get the number flops to implement step 2.

$$8rN^2m$$

Step 3, lowpass and decimation will require:

8 flops to do a complex multiply,
 m complex multiplies to create a lowpass filter output,
 N/m lowpass filter outputs per range bin after decimation,
 N/m rangebins per local scene and
 m^2 local scenes.

Multiply them all together to get $8N^2m$ flops to implement step 3.

The total computations for steps 2 and 3 is:

$$8*(r+1)*N^2m.$$

Computation Costs for 2-stage BP cont..

Next let us consider how much work it takes to back project to the smaller spot sizes using the outputs of the digital spotlight algorithms. If a scene size is reduced by a factor of m in both dimensions then the smaller scene has N^2/m^2 pixels. Because the digital spotlighting algorithm has reduced the PRF by a factor of m there are now N/m pulses, so for each image there are $(N/m)^3$ back projection operations required. Since we have m^2 patches the total number of backprojection operation is N^3/m . So the BP stage is pN^3/m .

The total number of flops for the DSBP is simply the sum of stage 1, digital spotlight and stage 2, back projection:

$$8(r+1)N^2m + pN^3/m$$

As a reminder in all the above equations:

N - diameter of full scene in pixels

m - number of taps in lowpass/decimation filter (also m^2 is the number of subpatches)

r - number of taps in recentering filter

Note that as m increases the N^3 term is reduced and the N^2 term increases.

For large N this will result in a net reduction in total computation.

Example

Relevant Example: Lets consider a 5 km spot at 1-foot (30 cm) resolution. $N = 16667$.
For this value of N the number of floating point operations for pure BP is

2.0e14 ($p=43$),

1.6e14 ($p = 35$),

and

0.6e14 ($p = 13$).

For the DSBP algorithm assume that $r = 6$.

Following Figure shows the ratio of BP to DSBP as a function of m for the 3 cases of p .

Maximum computational advantage occurs when $m^2 = pN / (8(r+1))$.

Note that improvements of over 50 times are achievable.

Example cont...

Computational
Advantage of DSBP⁴⁰
Over BP

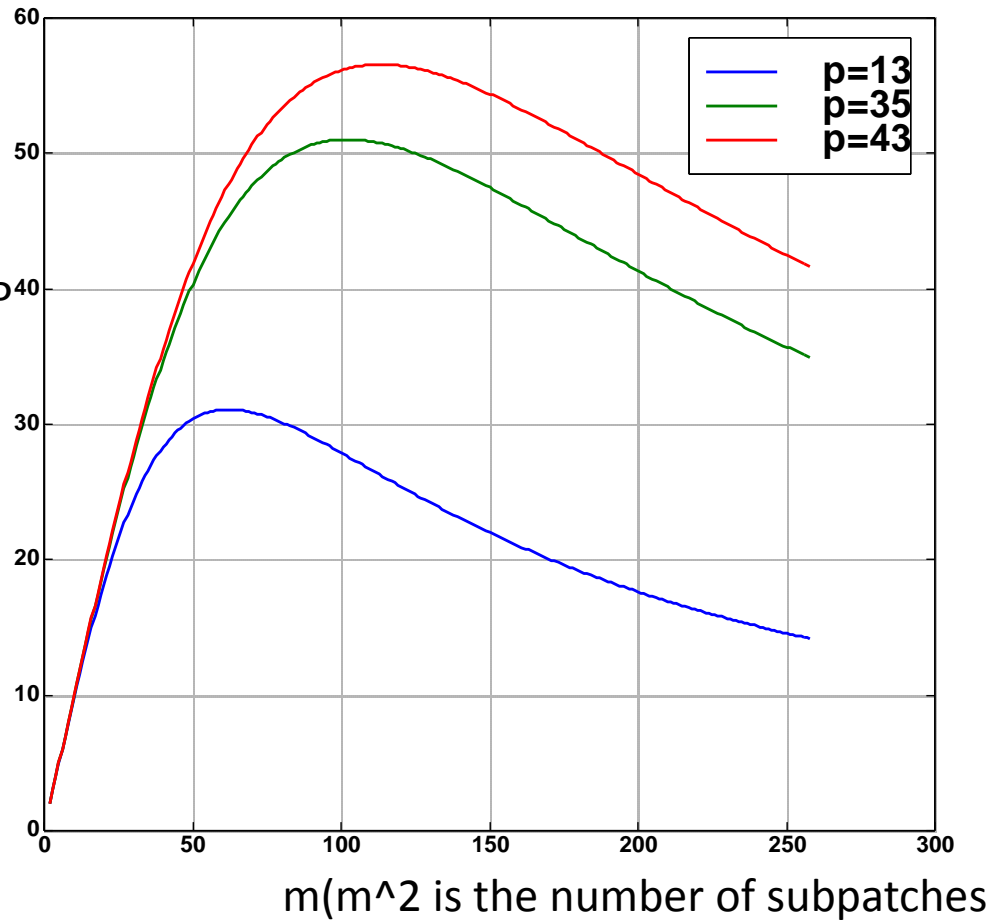
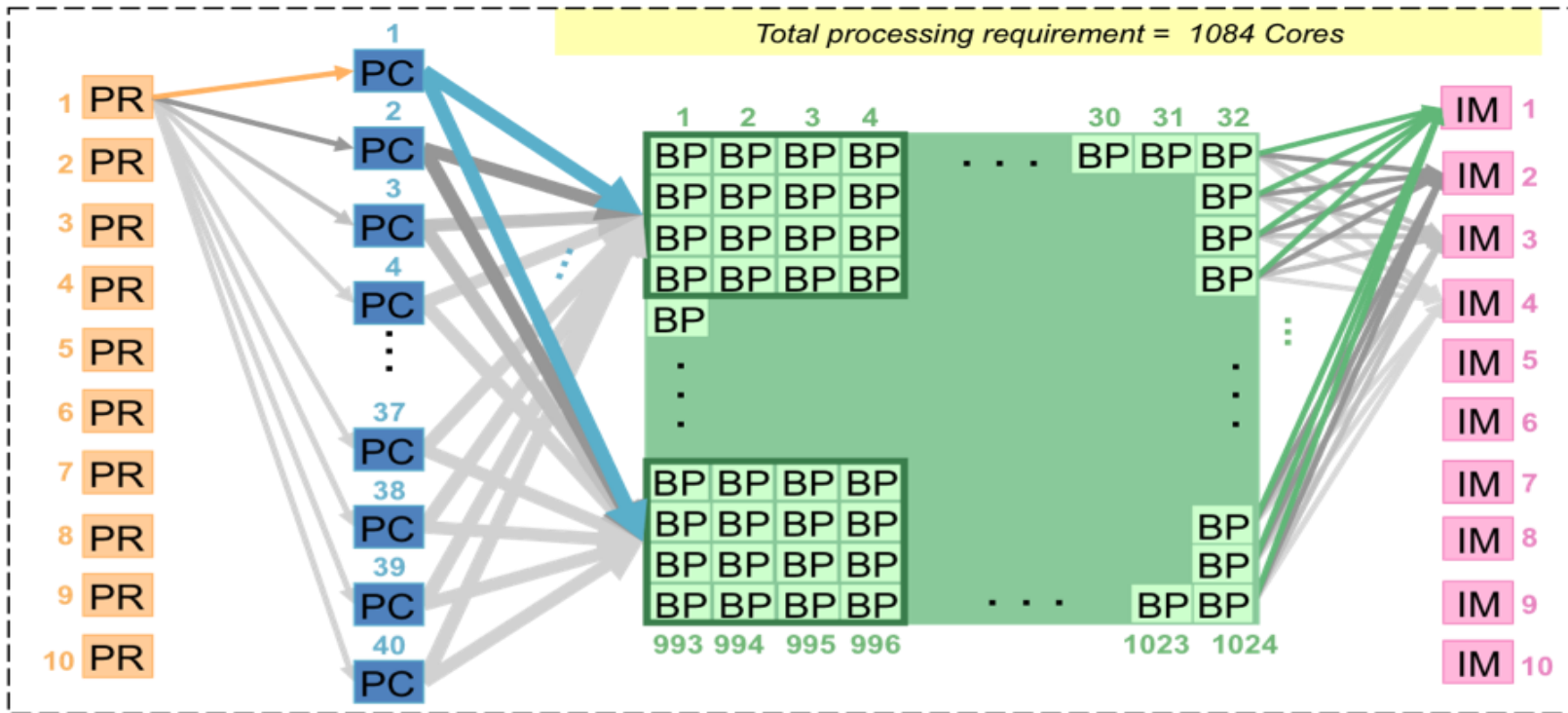


Figure 1 Ratio of flops required for back projection to flops required for digital spotlighting and back projection. m^2 is the number of subimages. p is the number of flops required to back project one pixel from one pulse. Image diameter = 5 km, Range resolution = 30cm.

Video SAR, Coherent and Non-Coherent Change Detection Processing

- Use Two Stage Backprojection for Video SAR First
- Non-Coherent Change Detection (NCD):
 - Amplitude only difference from two Passes SAR image.
 - This is good for vehicle sized targets and is robust to variations of collection geometry between the two passes
- Coherent Change Detection (CCD):
 - Amplitude and Phase difference from two Passes SAR Image.
 - Detect much smaller disturbances on the level of millimeters. CCD requires more processing and a tighter match between the two passes compared to non-coherent change detection. This layer shows footprints in a grassy field

Video SAR Processing



Each **PR core** reads a group of pulses from disk and distributes them to each **PC core** round robin.

Each **PC core** compresses a single pulse and broadcasts a portion of it to each **SuperChip group of BP cores**.

Each **BP core** performs azimuth presuming reducing the pulse rate by 100:1 and backprojects each of them. When a new subaperture is complete, it sends its tile of image data to the next **IM core** round robin.

Each **IM core** receives a tile of image data from all **BP cores** for an image and writes it to disk.

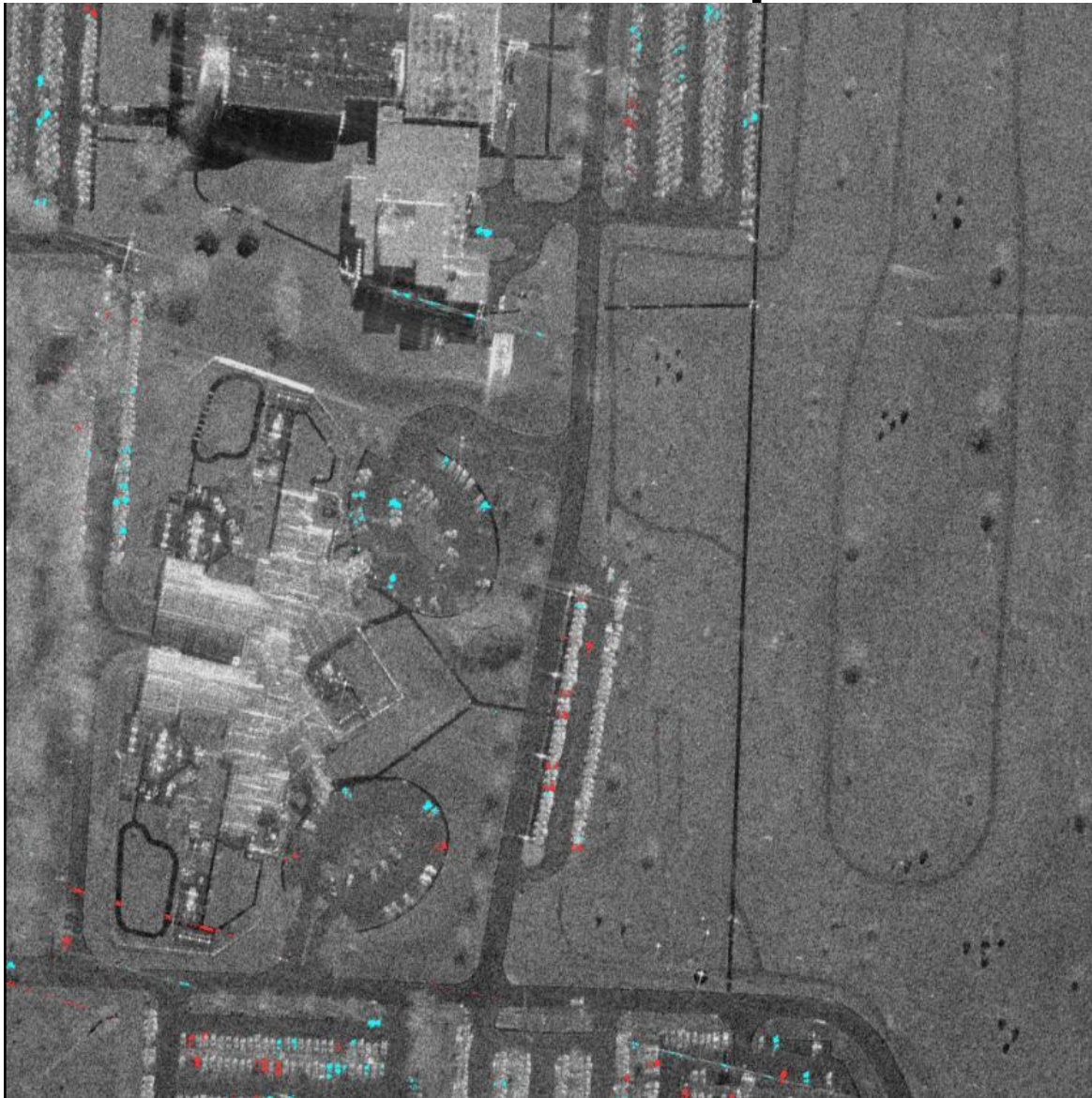
Two-Stage BP Implementation

Video SAR Example



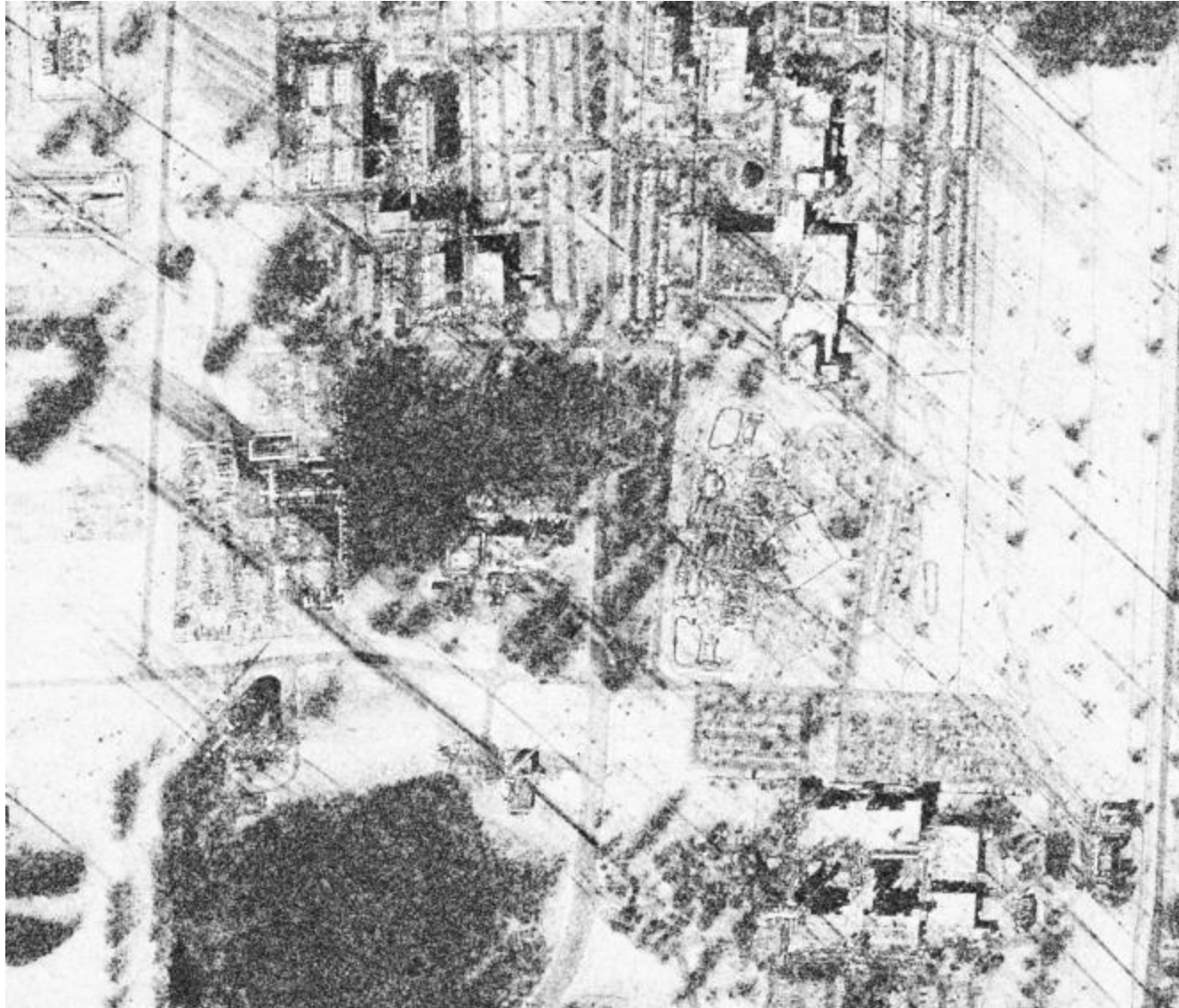
AFRL Public Release: 88 ABW-09-2007

NCD Example



AFRL Public Release: 88 ABW-09-2007

CCD Example



AFRL Public Release: 88 ABW-09-2007

3. Change Detection

Problem Statement

- **Objective:** Develop SAR signal processing algorithms to detect changes in scenes that are regularly interrogated by surveillance and reconnaissance radar platforms
- **Challenges:** Two or more SAR imagery are acquired at different time points. General problem of change detection in **delta-heading** multi-pass nonlinear SAR imagery corresponds to different slant planes of an interrogated scene; as a result one SAR image is a spatially-warped version of other SAR images, and their Doppler data are not identical.

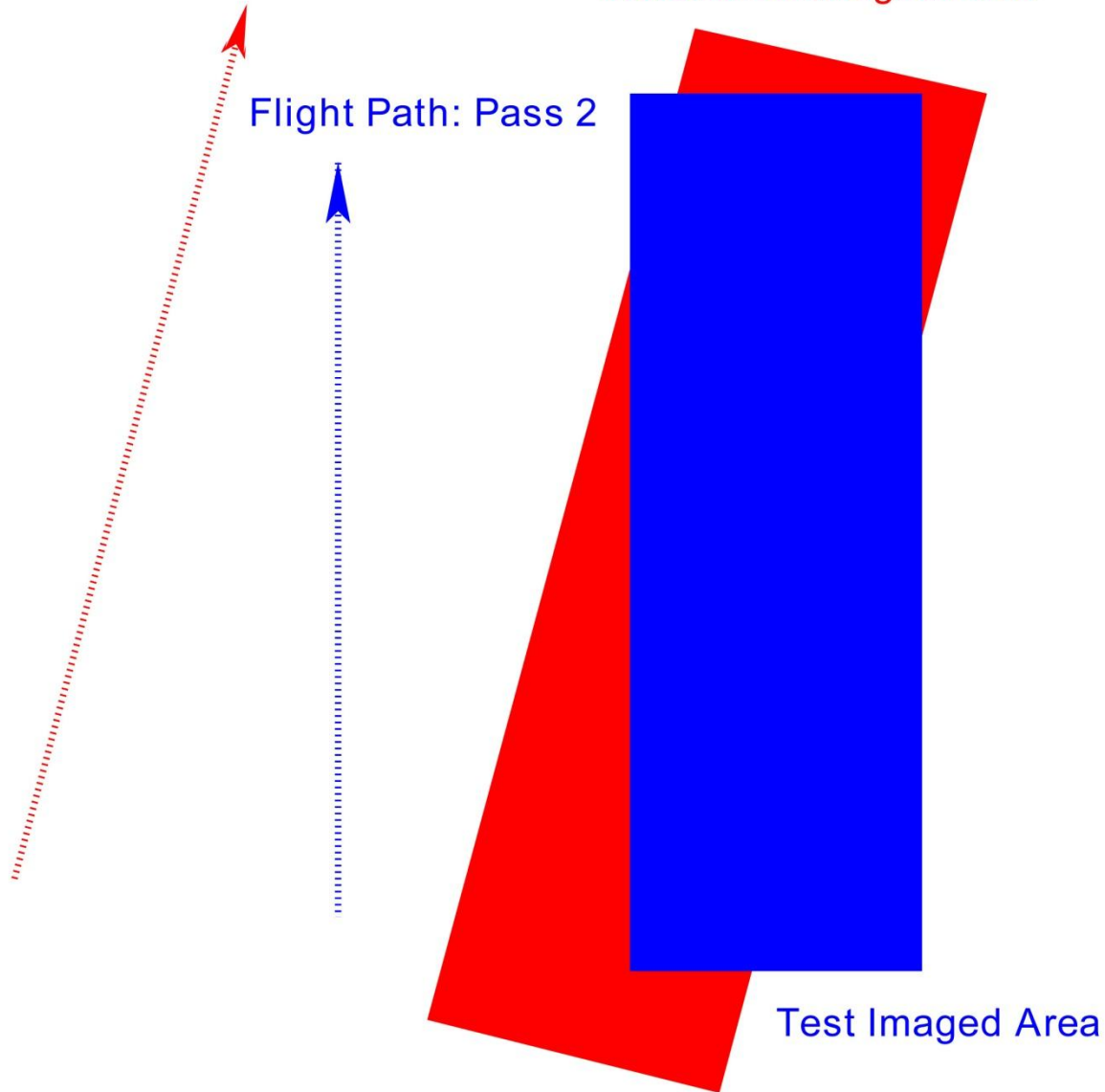
- **Approach:** Spatially and spectrally register these imagery such that a coherent processing of the resultant spatially and spectrally registered imagery could be exploited to detect subtle targets.
- Wavefront reconstruction or backprojection algorithm that is capable of spatially-varying motion compensation using INS data, and forming coherent ground UTM images for multiple SAR databases; this results in spatially-registered imagery.
- INS data are exploited for spectral registration of ground plane imagery. An adaptive filter is used to calibrate the multi-pass images with respect to the unknown phase, motion errors, INS errors and variations of the SAR system electronics.

Delta-Heading Multi-Pass SAR for CCD

Flight Path: Pass 1

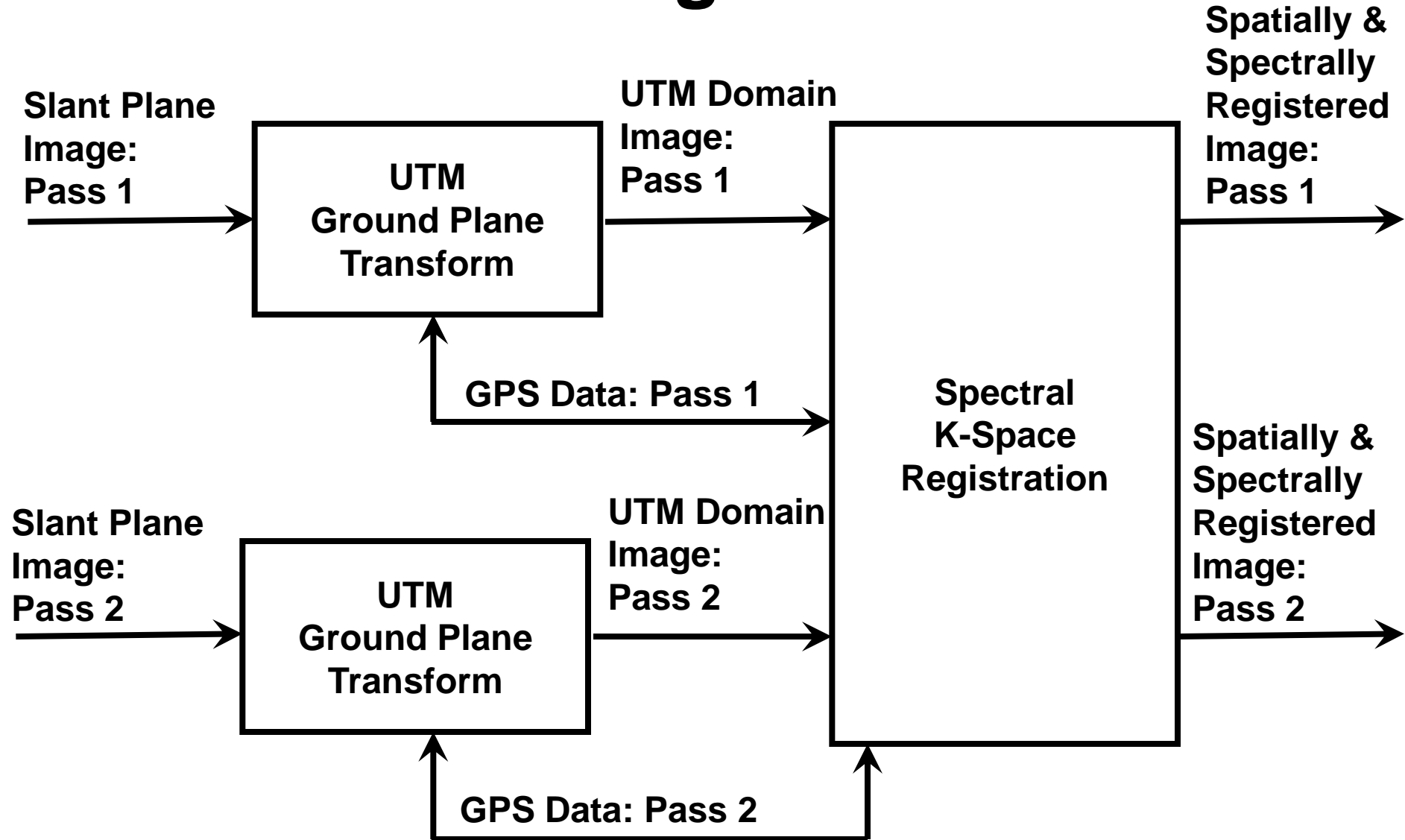
Reference Imaged Area

Flight Path: Pass 2



Test Imaged Area

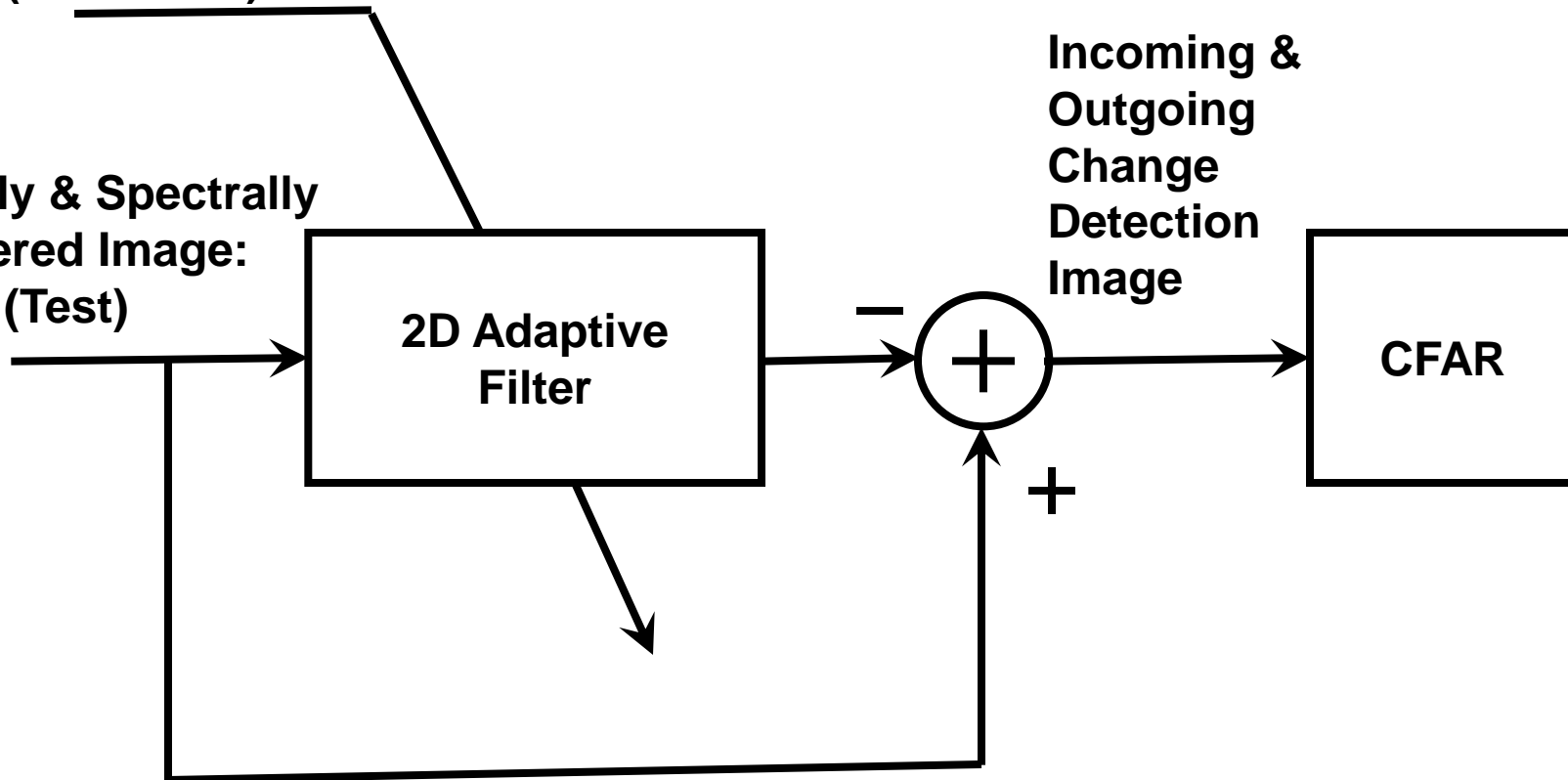
Signal Processing CCD Flowchart for Delta-Heading Multi-Pass SAR



CCD Flowchart for Delta-Heading Multi-Pass SAR, cont.

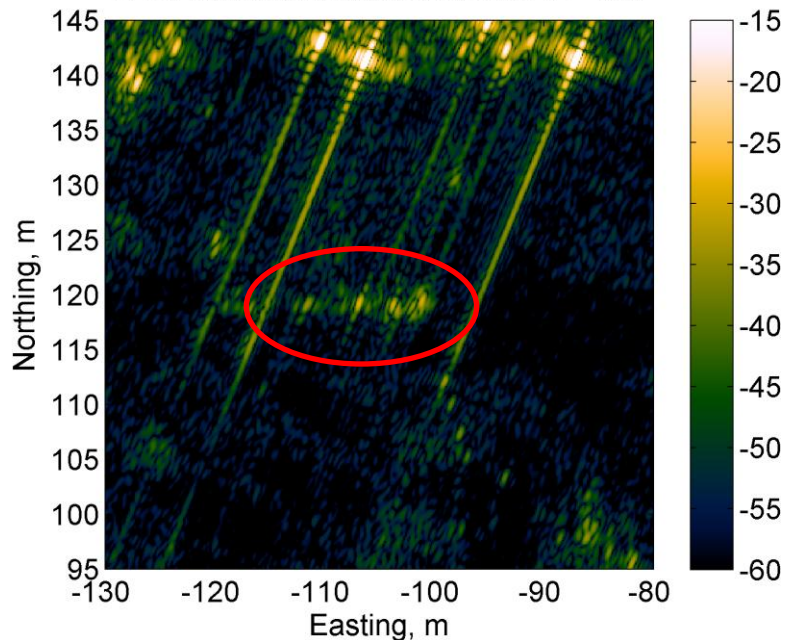
Spatially & Spectrally
Registered Image:
Pass 1 (Reference)

Spatially & Spectrally
Registered Image:
Pass 2 (Test)

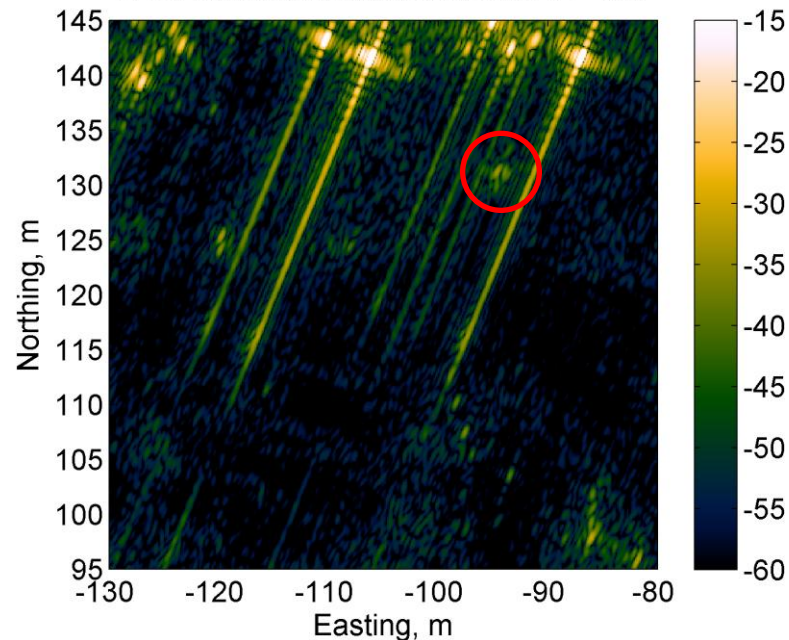


**Coherent Change Detection
Reconstructions:
FP-121 versus FP-128-1**

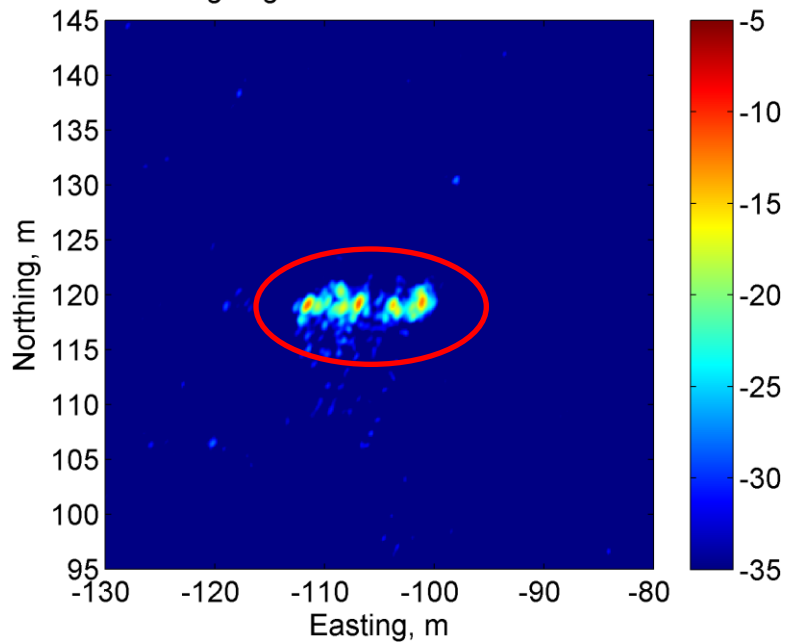
UTM Wavefront Reconstruction: FP-128



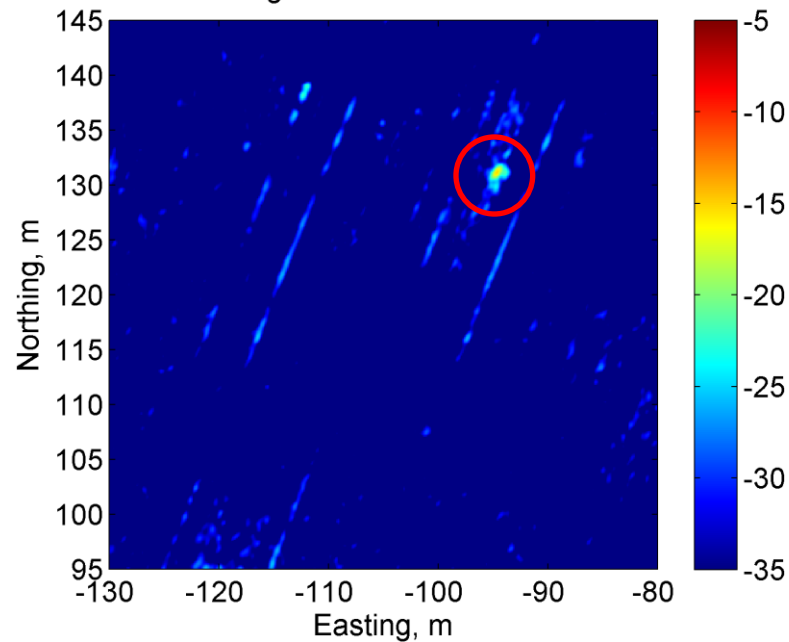
UTM Wavefront Reconstruction: FP-121



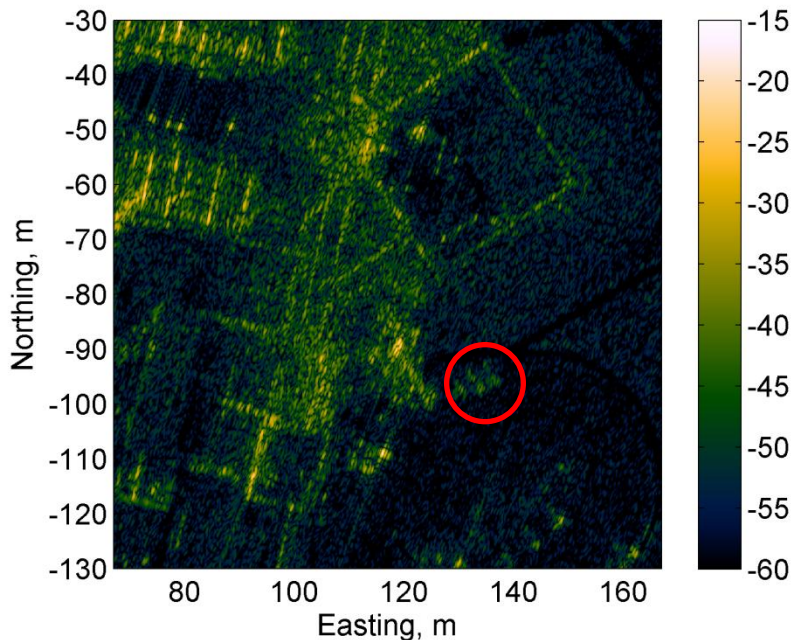
Outgoing CCD: FP-128 & FP-121



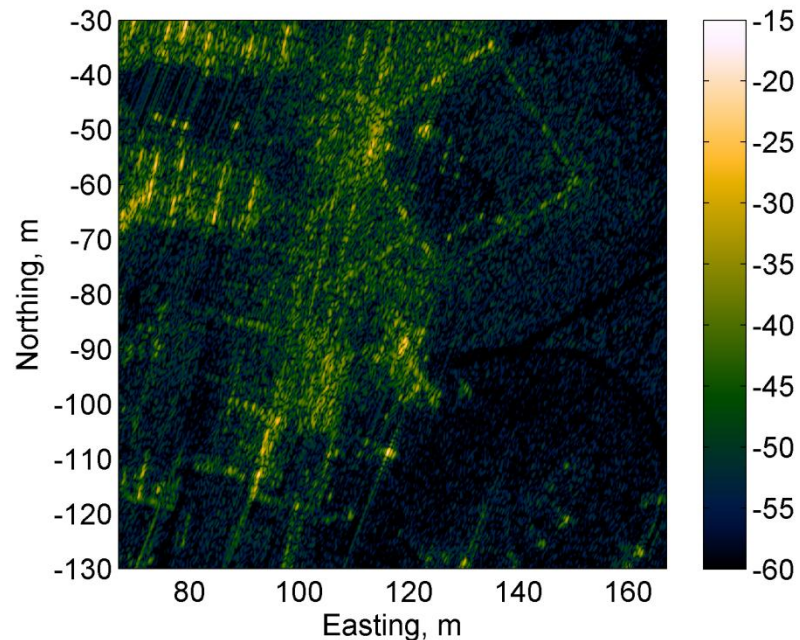
Incoming CCD: FP-128 & FP-121



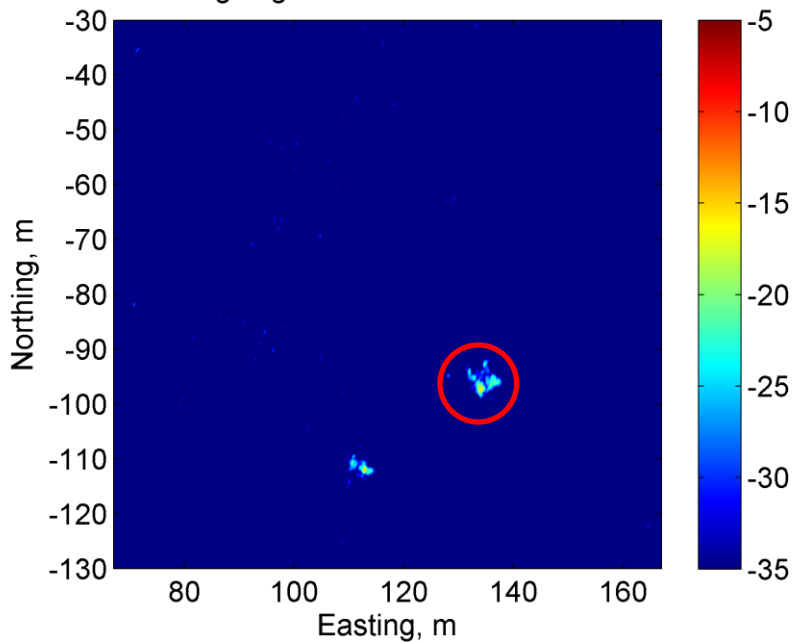
UTM Wavefront Reconstruction: FP-128



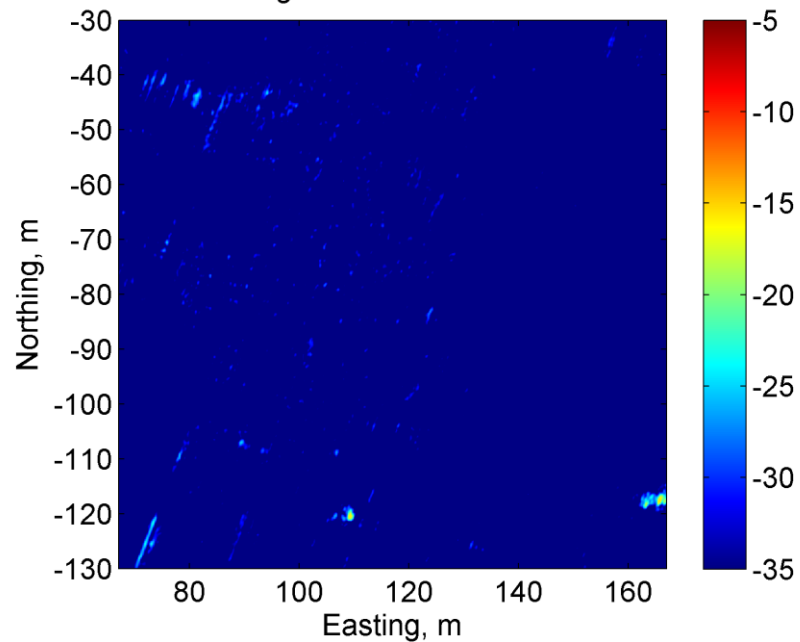
UTM Wavefront Reconstruction: FP-121



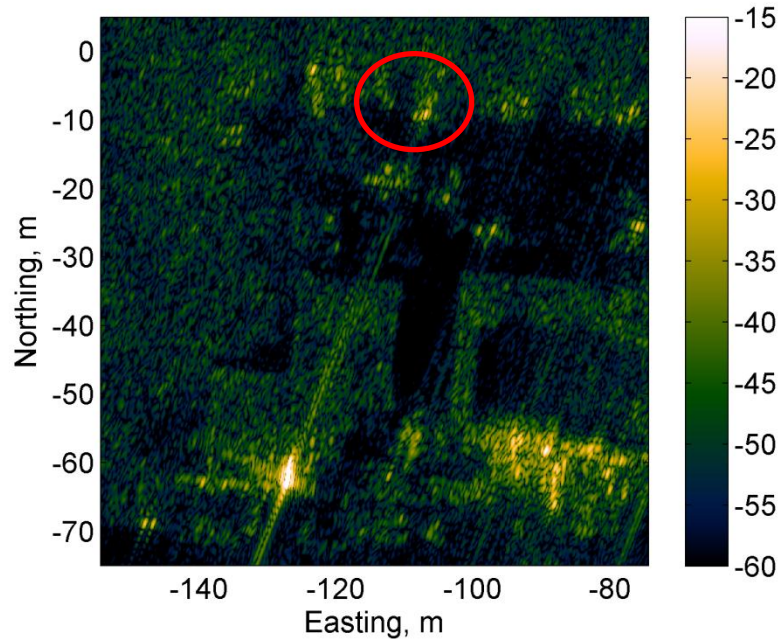
Outgoing CCD: FP-128 & FP-121



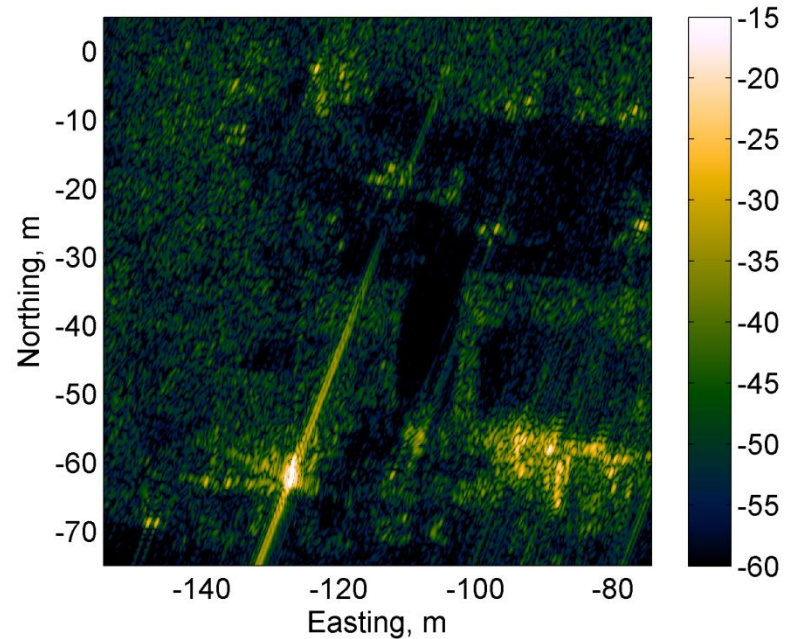
Incoming CCD: FP-128 & FP-121



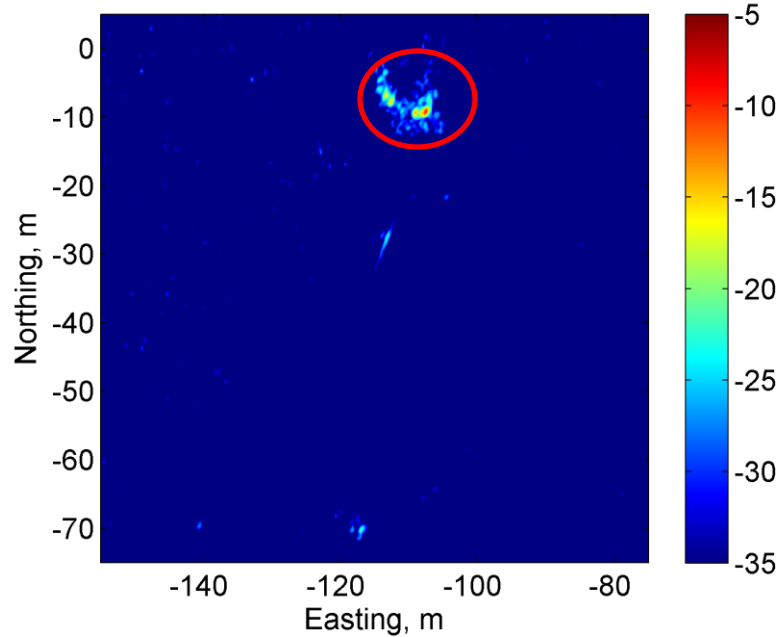
UTM Wavefront Reconstruction: FP-128



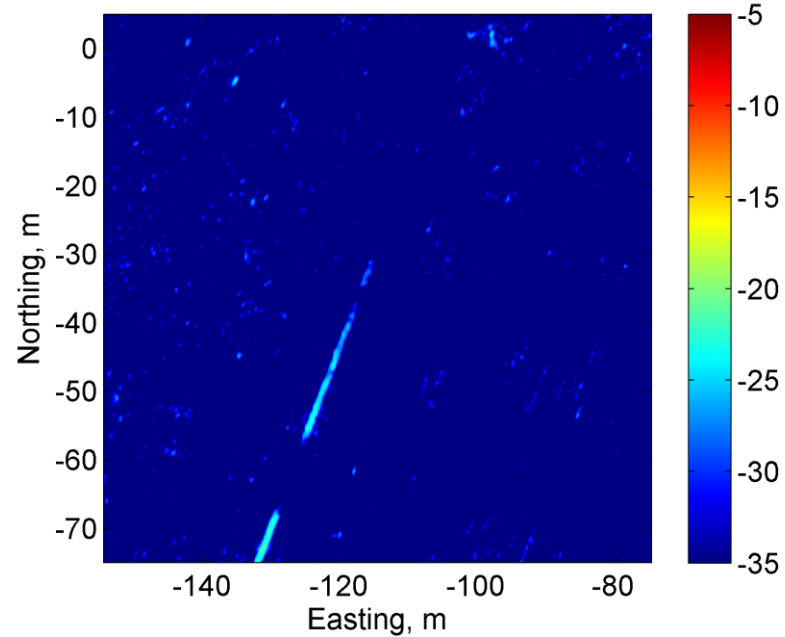
UTM Wavefront Reconstruction: FP-121



Outgoing CCD: FP-128 & FP-121



Incoming CCD: FP-128 & FP-121



4. Multiple Moving Target Detection and Tracking

4. Multiple Moving Target Detection and Tracking

Topics to be Covered

4.1 Objectives

4.2 Multiple Moving Targets Detection

**4.3 Multiple Moving Targets Association and
Tracking**

4.4 Ground Plane Geolocation

4.5 Application in Dismount Problem

4.1 Objectives

- **Detect** multiple moving targets in a heavy clutter (urban) environment using a single-pass with one or more along-track receivers and/or multiple-pass SAR
- **Associate** detections in **subaperture** SAR imagery to identify the radial-range and Doppler tracks of each target
- **Geolocate** each detected and tracked moving target using its subaperture radial-range and Doppler data with or without information on network of roads

4.2 Multiple Moving Targets Detection:

Possible Databases

- SAR-MTI is constructed using a 2D adaptive change detection algorithm
- Three types of databases (options) to form *Reference* and *Test* images:
 - I. Subaperture monostatic and along-track bistatic (DPCA) monopulse SAR data from a single pass (coherent change detection)
 - II. Subaperture monostatic SAR data of a single pass (noncoherent change detection ... coherent CD is also possible)
 - III. Subaperture monostatic SAR data of multiple passes (coherent change detection)

- Why *subaperture*-based processing?
- For an IR or visible camera, a moving target appears: a) slightly blurred but still detectable via change detection in an image sequence; & b) around its true spatial coordinates (on camera's focal plane)
- In a full-aperture (-resolution) SAR image: a) to say a moving *vehicle* signature appears blurred is an understatement; & b) the mover signature would be Doppler-shifted
- In a subaperture SAR image, a mover would be more localized for detection purposes though still Doppler-shifted

- ***Option I***, also called SAR DPCA-MTI, is effective when the moving target phase variations in the two receiver channels are detectable despite noise, etc., e.g., targets moving non-parallel to the flight path or dismounts (noise analysis shown later); this approach can detect targets whose signatures are buried under clutter
- ***Options II and III***, in theory, could detect targets moving parallel to the flight path; however, a moving target signature has to be at or above clutter for detectability

Adaptive Filtering for Reference-Test Image Calibration

- 2D Adaptive filtering method (called Signal Subspace Processing, SSP) compensates for
 1. Unknown variations of the electronics, antennas, etc. of the two SAR databases
 2. Spatial warping in the test and reference imagery due to unknown INS errors and/or unknown variations in target area height
- Interferometric (phase only) processing for change detection could also benefit from adaptively calibrated imagery

Local SSP

- A realistic miscalibration model for the two receiver channels is based on the fact that the **filter is spatially-varying**. In this case, the relationship between the test and reference images can be expressed via the following:

$$\hat{f}_{RT}(x, y) = \int f_R(x - u, y - v) h_{xy}(u, v) du dv$$

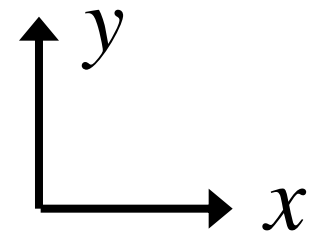
where in this model the filter $h_{xy}(u, v)$ varies with the spatial coordinates (x, y)

- While the above model is a more suitable one, however, it is computationally prohibitive to implement the LMS or SSP method for this scenario.
- A practical alternative is to assume that the filter is approximately spatially-invariant within a small area in the spatial domain.
- In this case, we can divide the imaging scene into subpatches within which the filter can be approximated to be spatially-invariant.

LSSP

Subpatch
Number ℓ
is centered
at (x_ℓ, y_ℓ)

Solution of
2D Adaptive
Filter is
Assigned to
This Grid
Point



- The resultant model for a subpatch is

$$\begin{aligned}\hat{f}_{RT\ell}(x, y) &= f_{R\ell}(x, y) \otimes h_{\ell}(x, y) \\ &= \int f_{R\ell}(x - u, y - v) h_{\ell}(u, v) du dv\end{aligned}$$

where ℓ represents an index for the subpatches.

- In this approach, that we call ***Local Signal Subspace Processing*** (LSSP), the LMS/SSP method is used to estimate the local unknown calibration filter $h_{\ell}(u, v)$

Global SSP

- After the calibration filter is estimated for each subpatch, an approach that we call ***Global Signal Subspace Processing*** (GSSP) is used to estimate the original spatially-varying filter $h_{xy}(u, v)$ and the calibrated reference image (that is, estimate of the test image) via

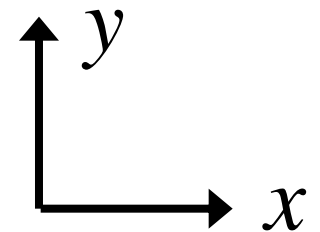
$$\hat{f}_{RT}(x, y) = \int f_R(x - u, y - v) h_{xy}(u, v) du dv$$

- Available samples of 2D adaptive filter for the subpatches $h_\ell(u, v)$ are at the grid point (x_ℓ, y_ℓ) ; these are shown as blue dots.
- For every (u, v) (that is the 2D filter domain), the values of the 2D spatially-varying filter $h_{xy}(u, v)$ are interpolated on the original image grid in the spatial domain (x, y) (black dots) from the available filter samples $h_\ell(u, v)$ at the grid points (x_ℓ, y_ℓ) (blue dots).

GSSP

Available
Samples
are in Blue

Interpolated
Points are
in Black

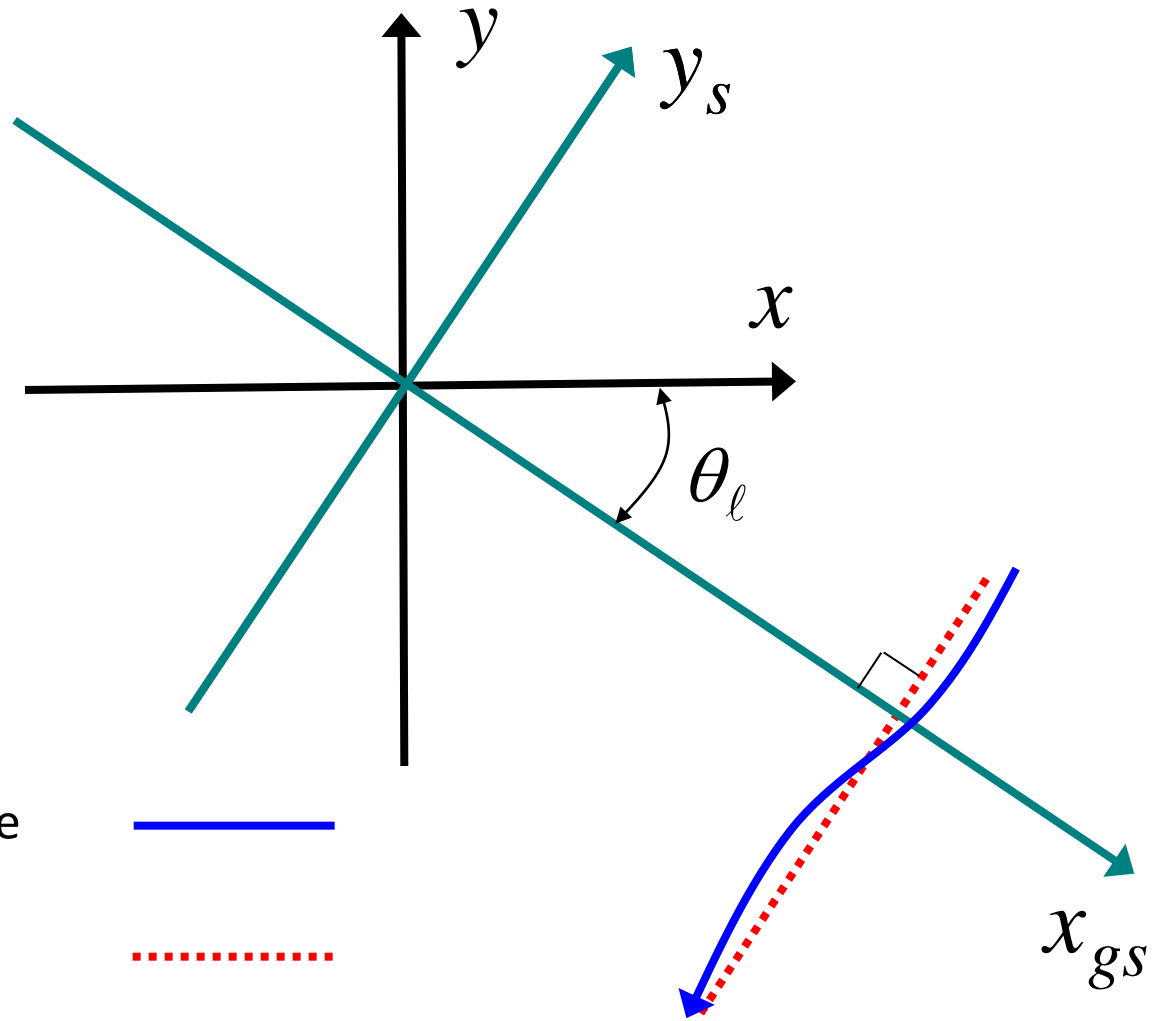


SAR-MTI Using Monostatic and Along-Track Bistatic Monopulse Configuration
(DPCA-MTI, Option 1)

Symbols

- 3D spatial domain: (x, y, z)
- Northing and Easting (UTM) domain: (x, y)
- Target area mean elevation: Z_{target}
- Subaperture number: ℓ
- Radar coordinates at midpoint of subaperture:
$$\left(X_{\text{radar}}^{(\ell)}, Y_{\text{radar}}^{(\ell)}, Z_{\text{radar}}^{(\ell)} \right)$$
- Constant velocity of synthesized linear subaperture:
$$\left(v_{x\text{radar}}^{(\ell)}, v_{y\text{radar}}^{(\ell)}, v_{z\text{radar}}^{(\ell)} \right)$$
- Synthesized flight path motion angle: θ_{ℓ}
- Slant-plane ground range: $x_{gs} = x \cos \theta_{\ell} + y \sin \theta_{\ell}$

Imaging System Geometry: Top View



Nonlinear Subaperture



Synthesized Linear
Subaperture



- Slant-plane: $(x_s^{(\ell)}, y_s^{(\ell)})$

- Slant-plane range:

$$x_s = \sqrt{x_{gs}^2 + (Z_{\text{radar}}^{(\ell)} - Z_{\text{target}})^2}$$

- Slant-plane cross-range:

$$y_s = -x \sin \theta_\ell + y \cos \theta_\ell$$

- Monostatic slant-plane subaperture SAR image:

$$f_{\text{mono}}^{(\ell)}(x_s, y_s)$$

- Bistatic slant-plane subaperture SAR image:

$$f_{\text{bist}}^{(\ell)}(x_s, y_s)$$

- Slant-plane subaperture GSSD-MTI image:

$$f_{\text{MTI}}^{(\ell)}(x_s, y_s)$$

- UTM domain image transforms:

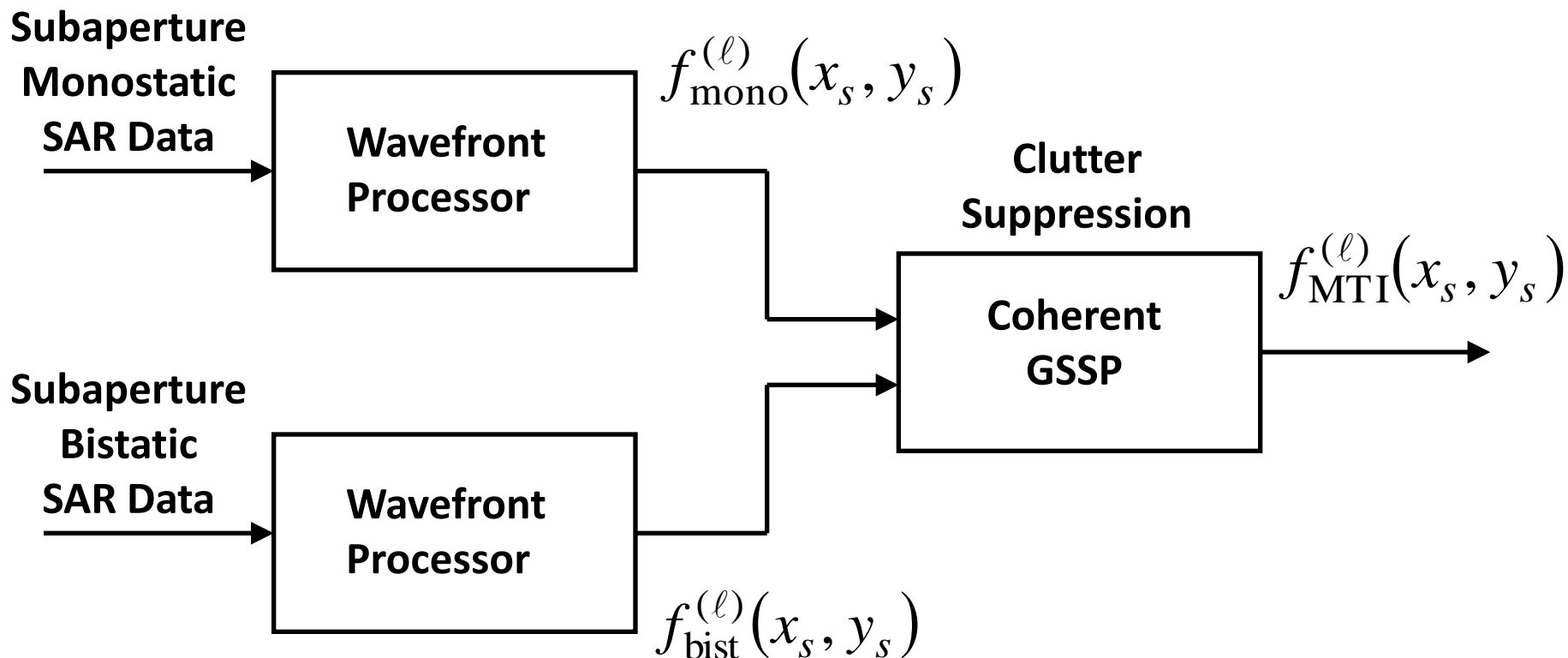
$$f_{\text{mono}}^{(\ell)}(x_s, y_s) \Rightarrow g_{\text{mono}}^{(\ell)}(x, y)$$

$$f_{\text{MTI}}^{(\ell)}(x_s, y_s) \Rightarrow g_{\text{MTI}}^{(\ell)}(x, y)$$

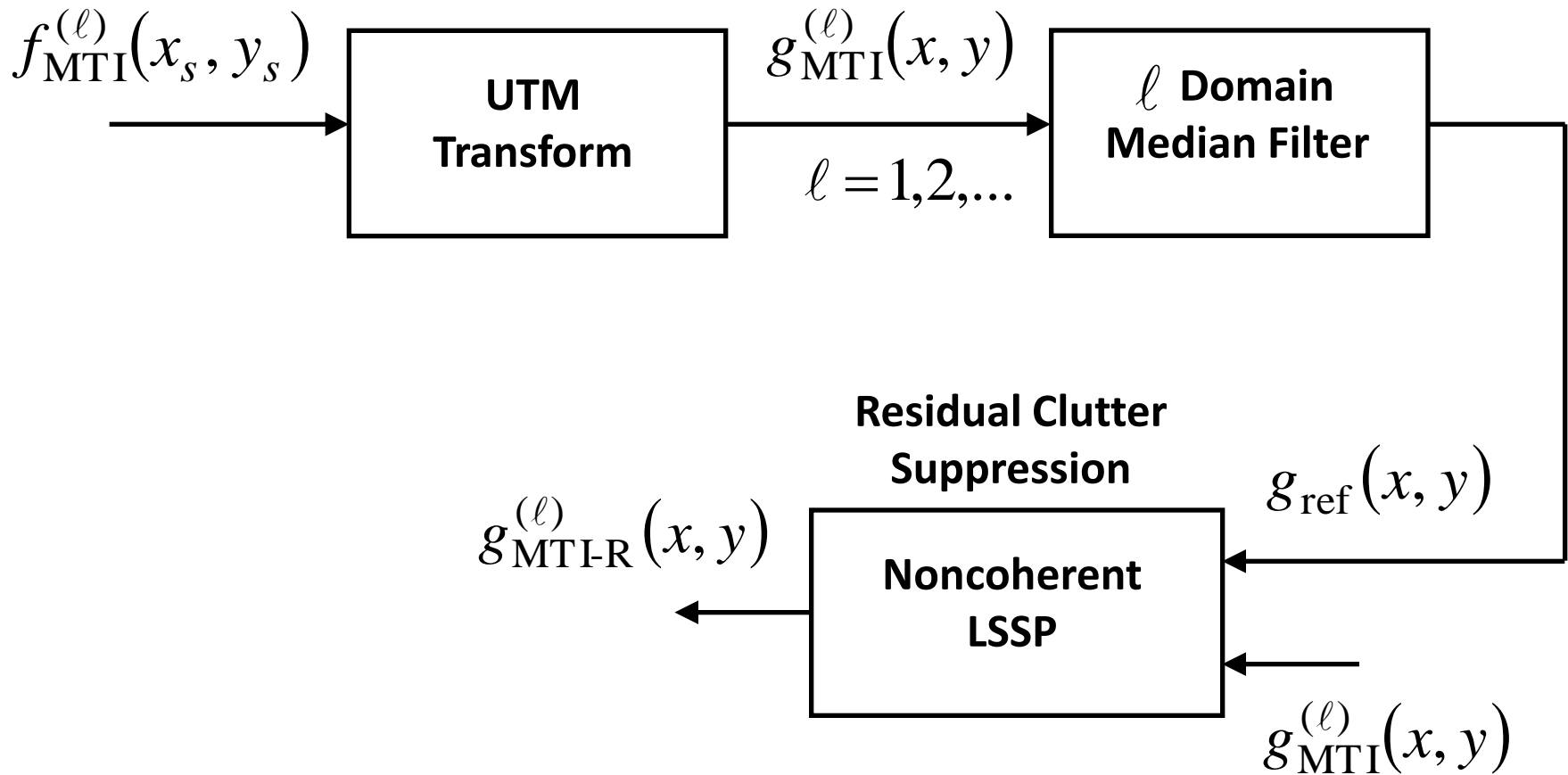
- UTM domain SAR-MTI image after residual clutter suppression:

$$g_{\text{MTI-R}}^{(\ell)}(x, y)$$

Coherent Clutter Suppression Using GSSP on Slant-Plane



UTM Transform and Residual Clutter Suppression on Ground Plane



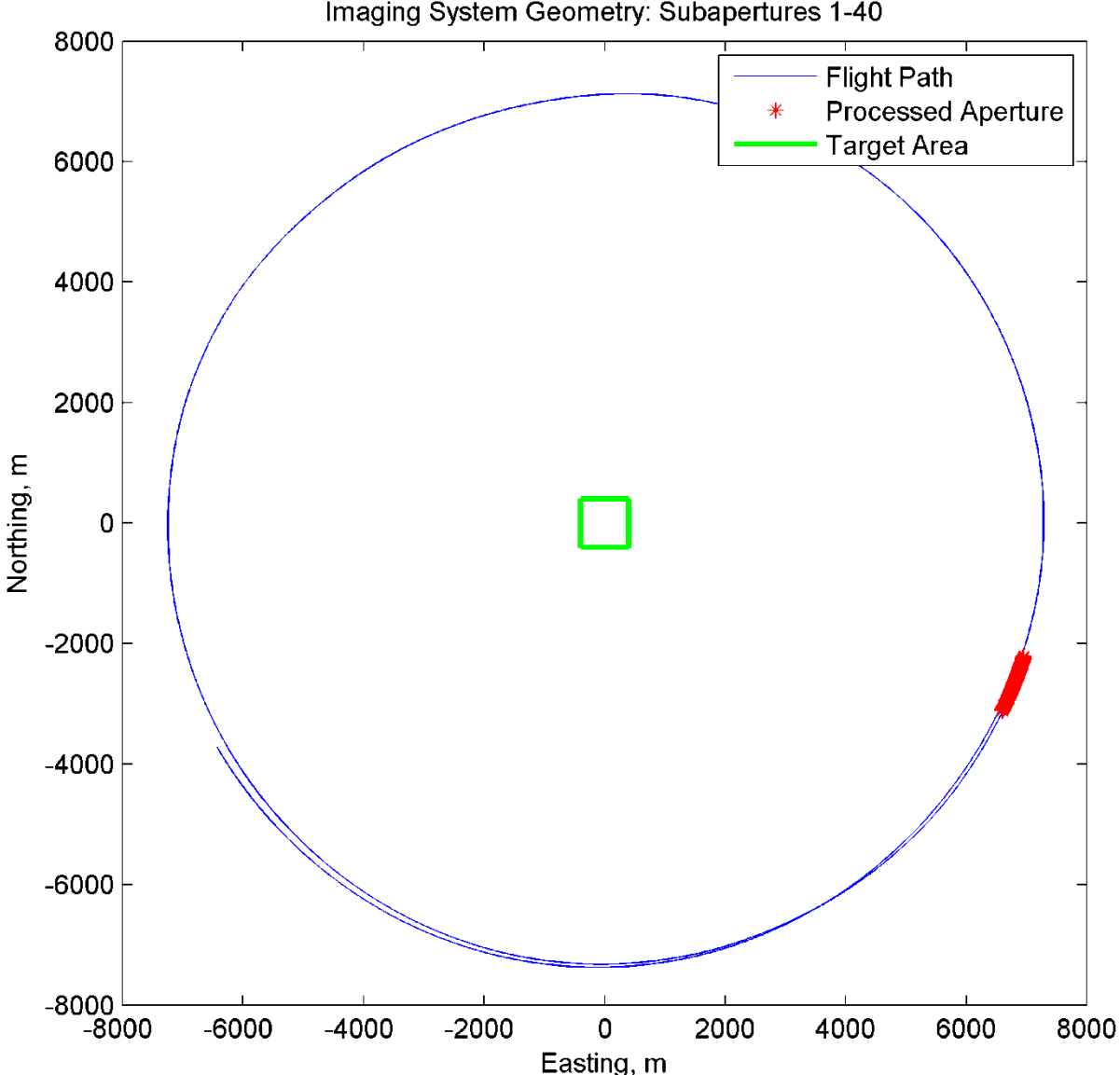
Results with SAR Data

Subaperture Processing:

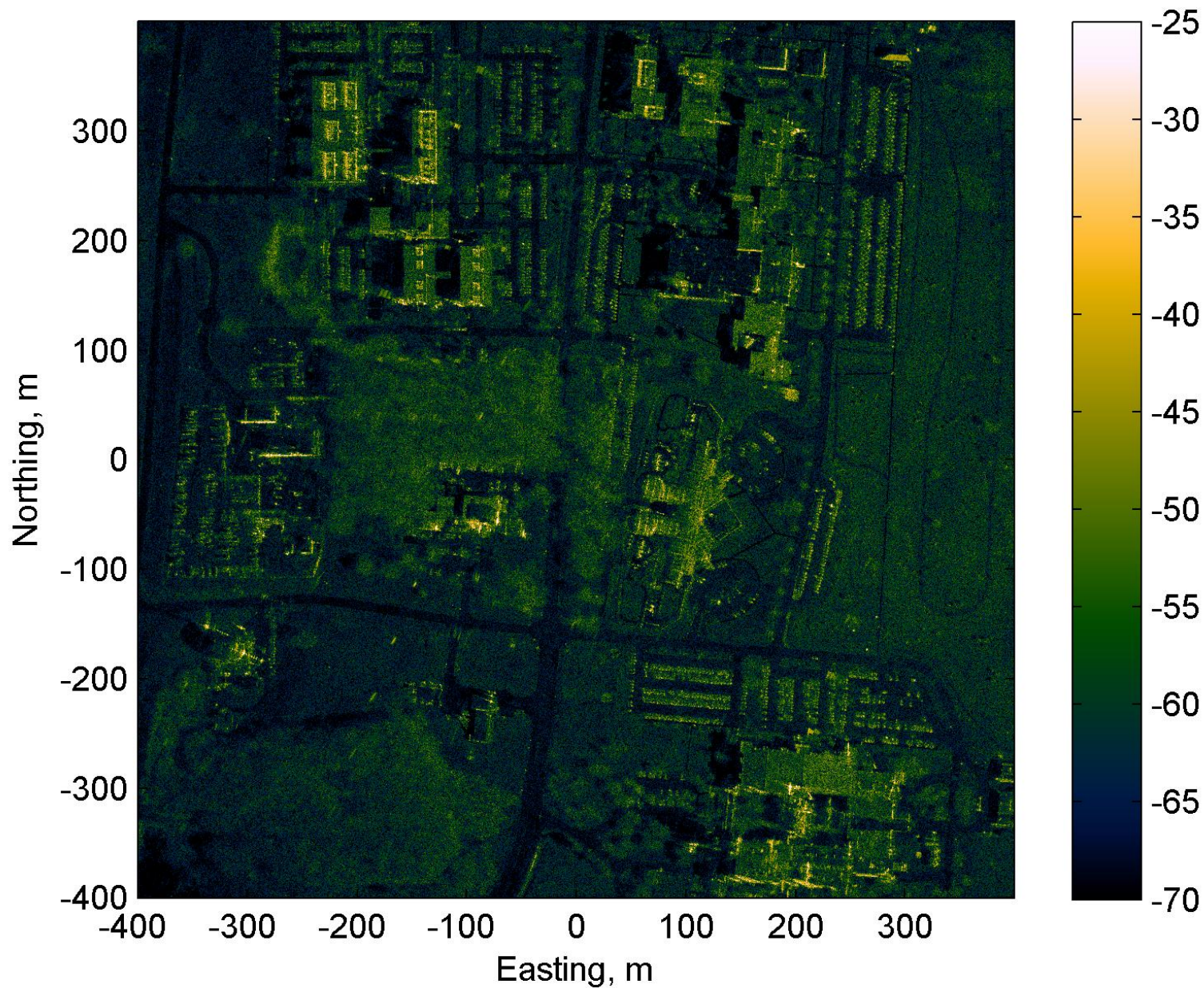
1024 PRIs (.5 sec) per Subaperture

**512-PRI Overlapping Subapertures (.25
sec updating)**

Imaging System Geometry: Subapertures 1-40

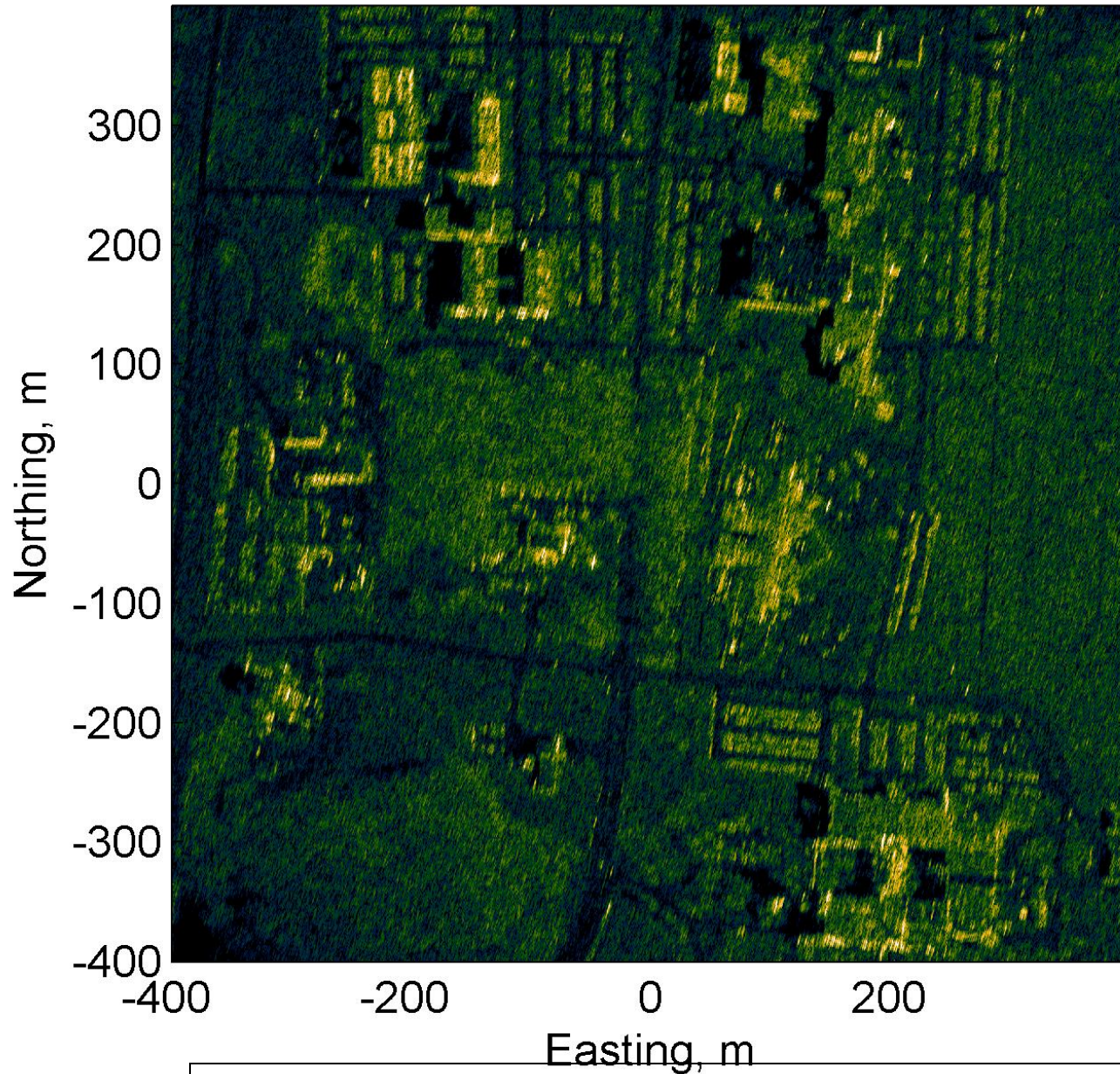


Full-Aperture Reconstruction



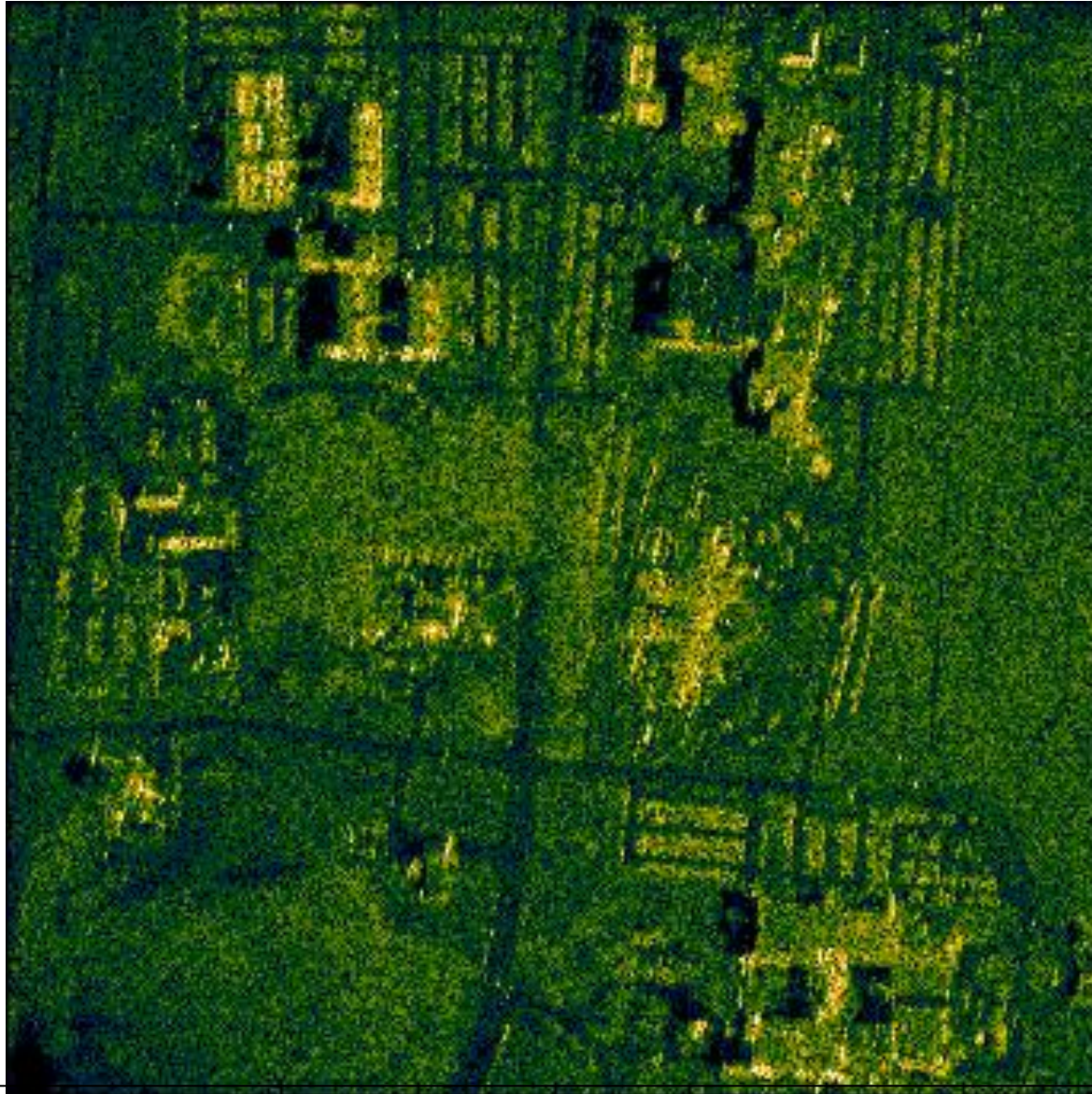
Public Release: Document Number 88 ABW-10-0809

Subaperture Reconstruction



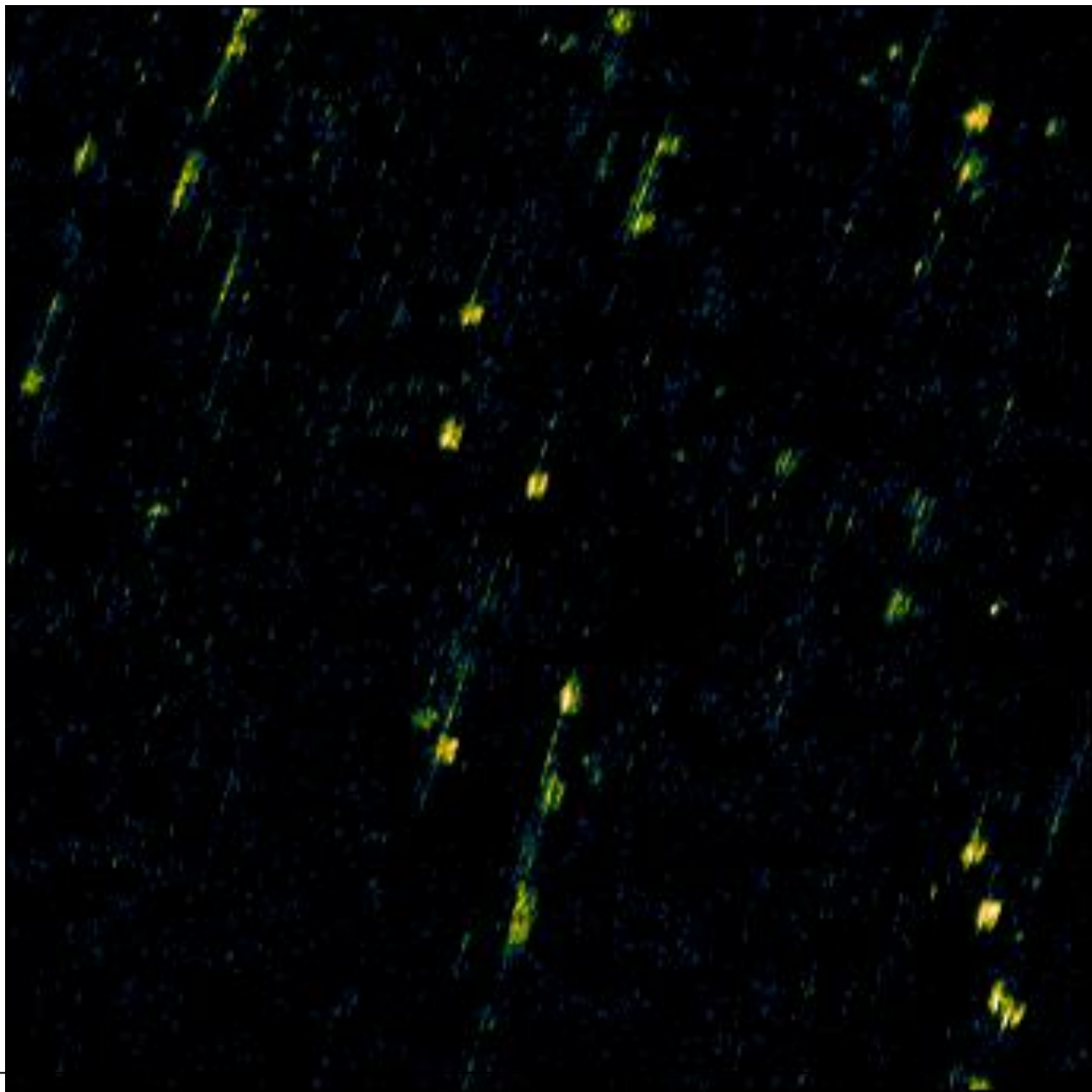
Public Release: Document Number 88 ABW-10-0809

Subaperture Reconstructions: 1-540



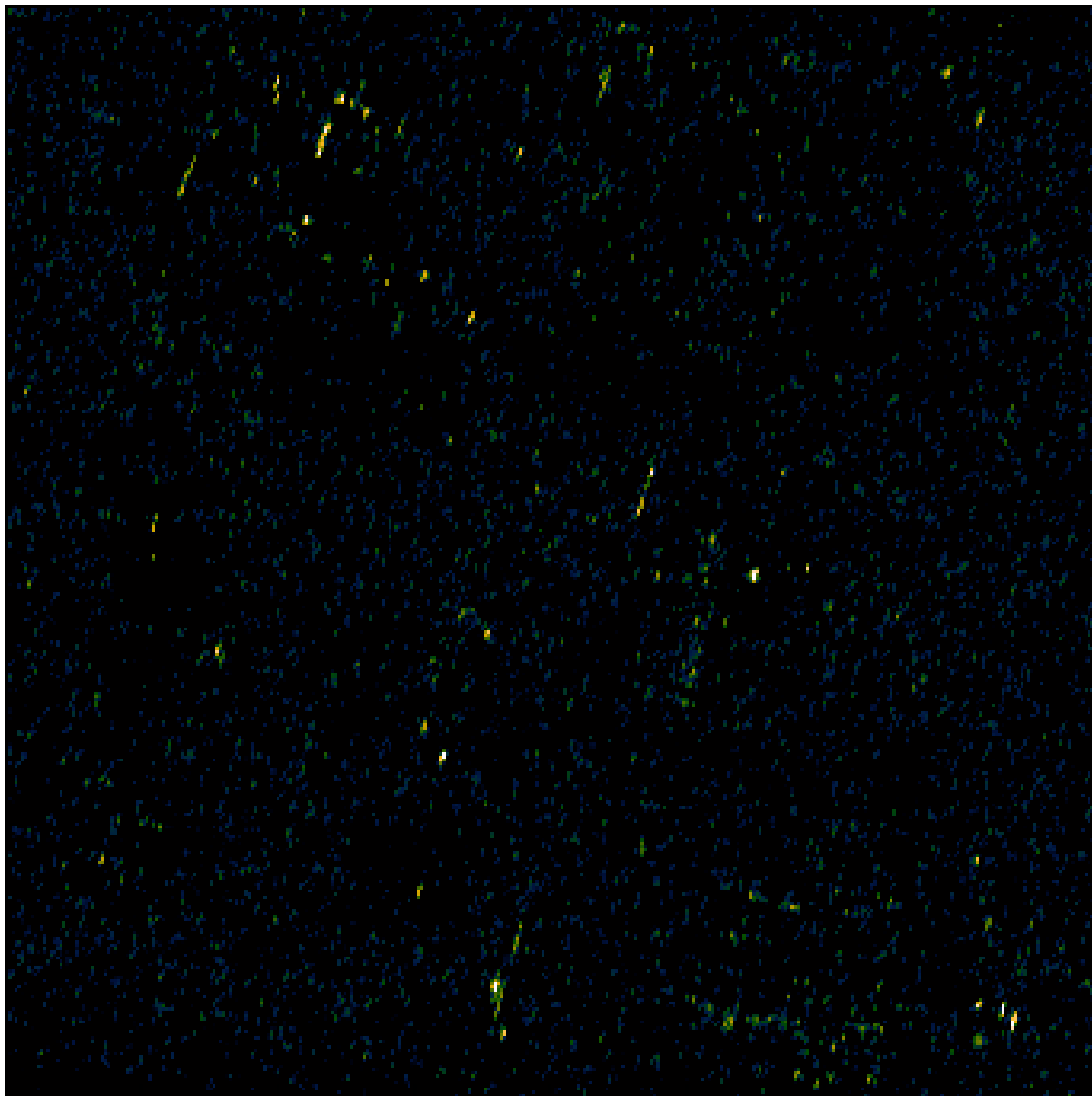
Public Release: Document Number 88 ABW-10-0809

**MTI Detections:
Coherent Single Pass
Dual Receivers
(DPCA-MTI, Option 1)**

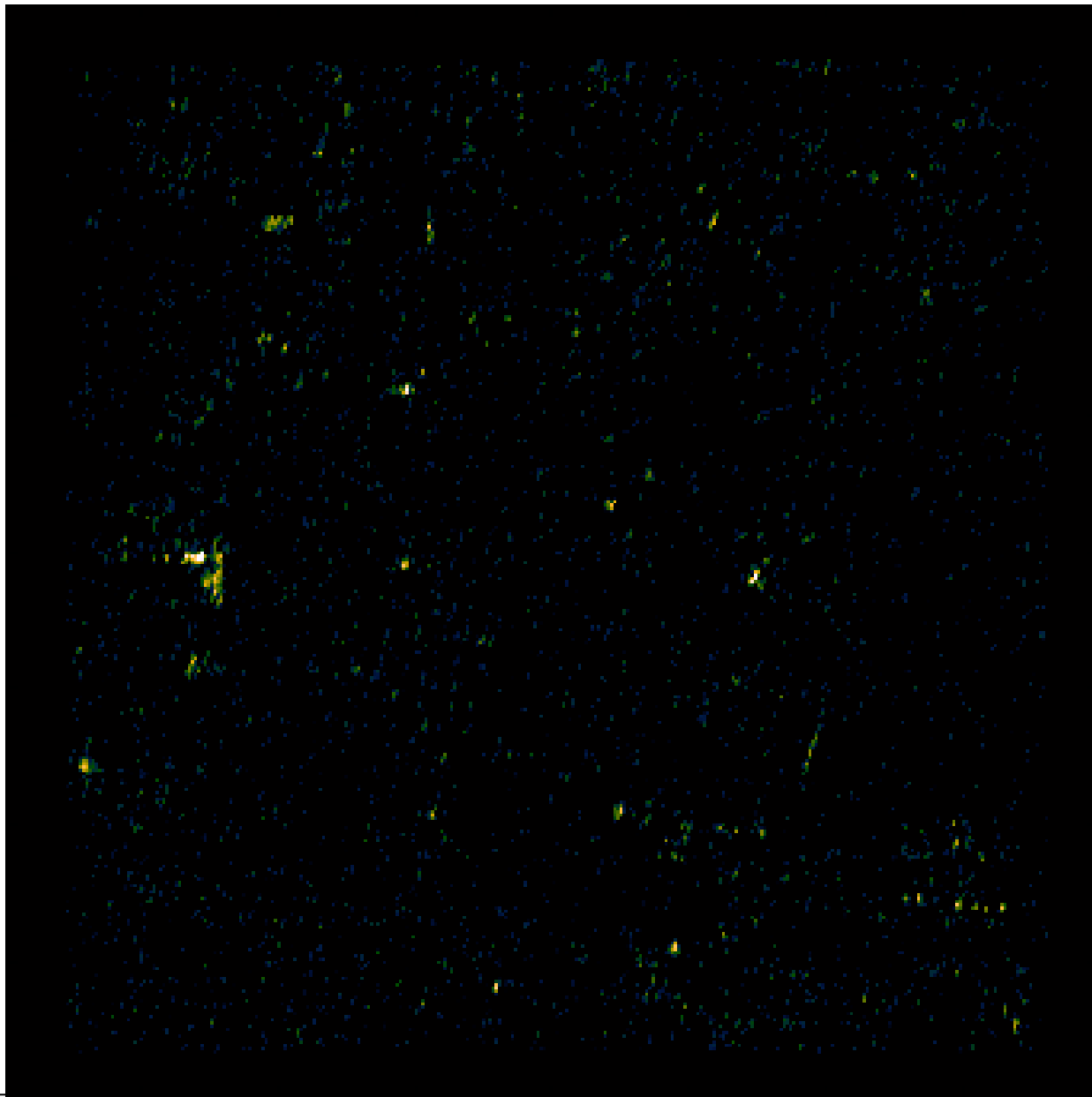


Public Release: Document Number 88 ABW-10-0809

**MTI Detections:
Noncoherent Single
Pass Single Receiver
(Option 2)**



**MTI Detections:
Coherent
Dual Pass
(119 & 128)
(Option 3)**



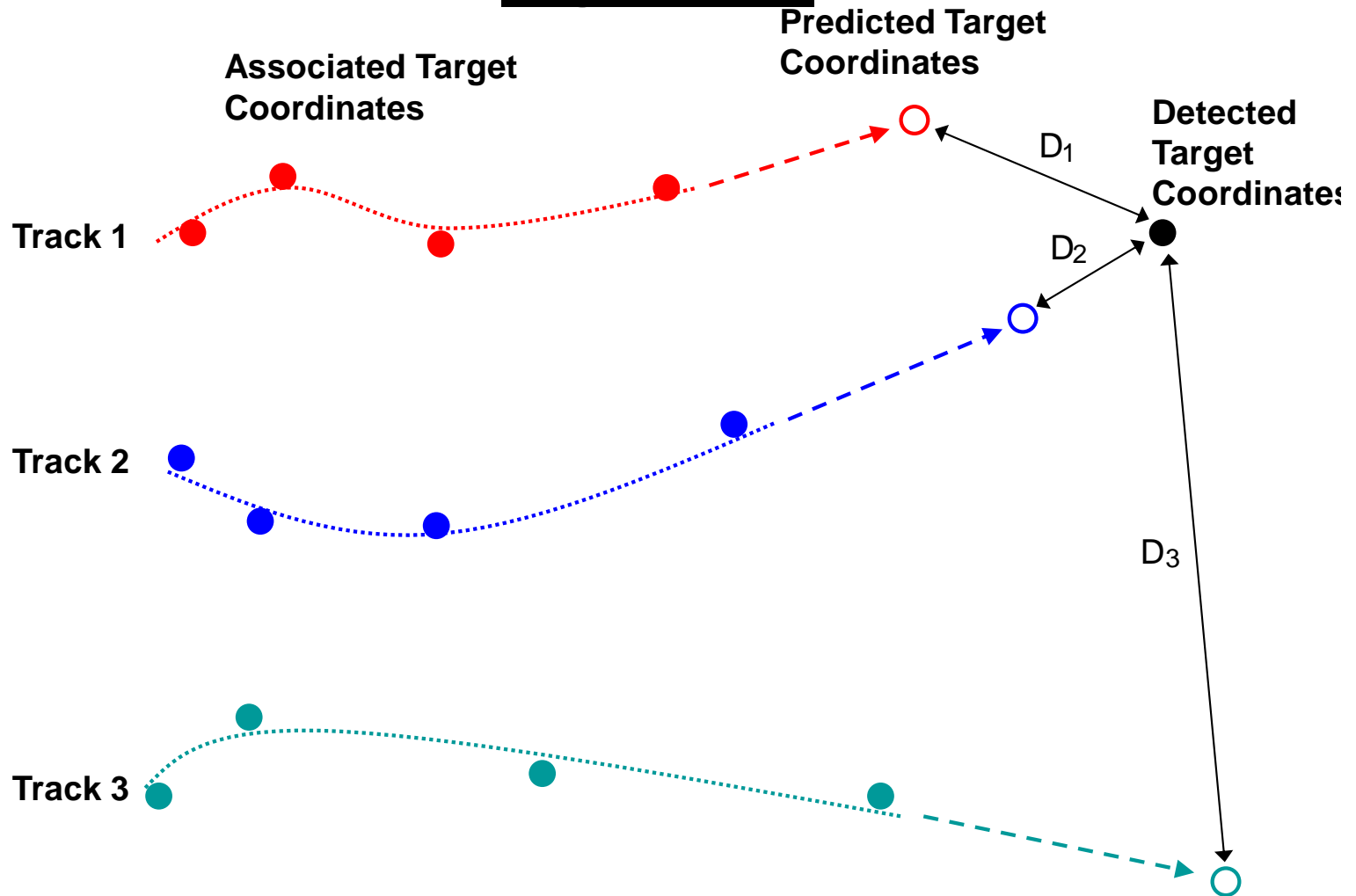
Public Release: Document Number 88 ABW-10-0809

4.3 Multiple Moving Targets Association And Tracking

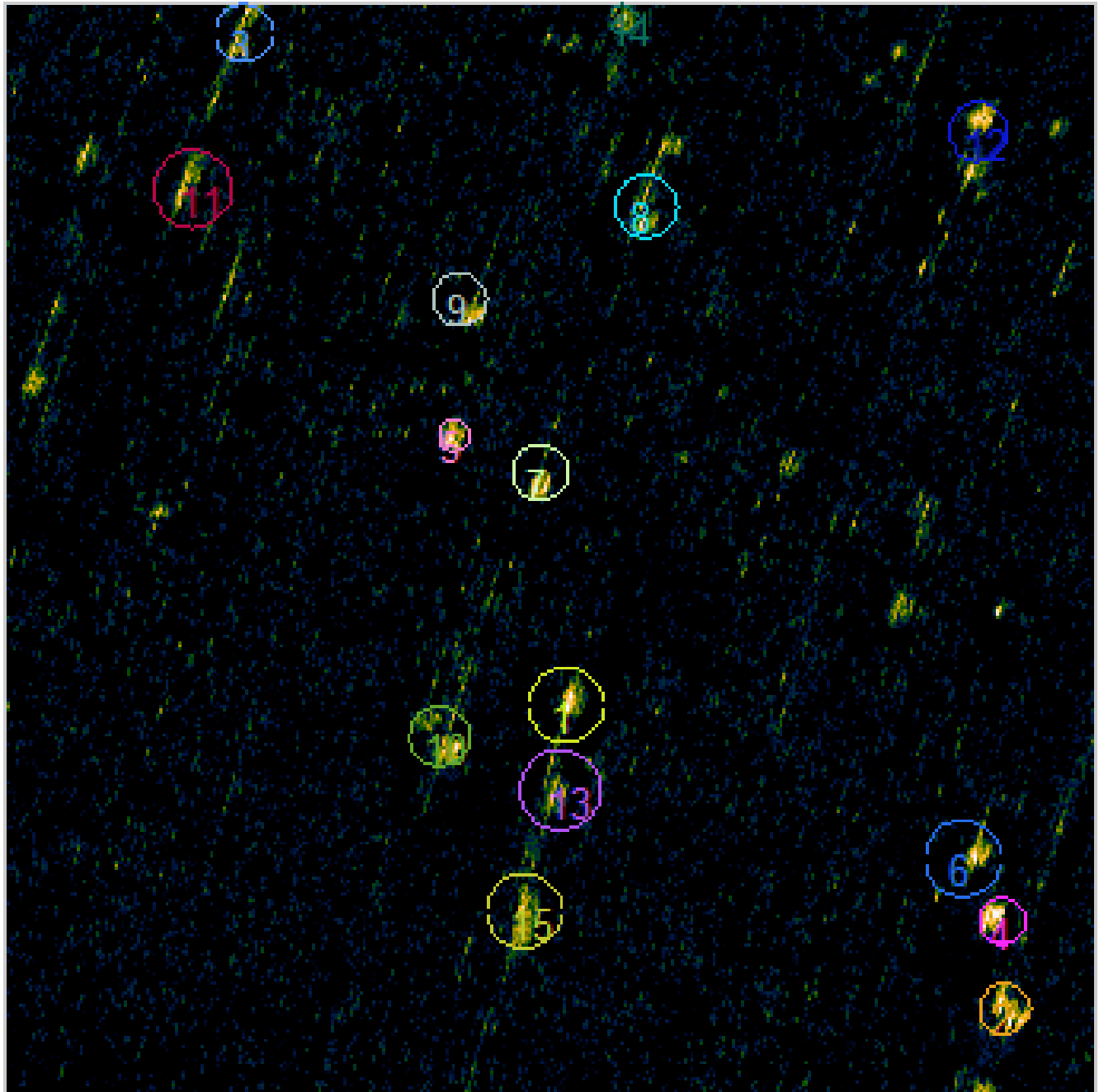
- An algorithm that uses linear prediction to associate MTI hits in IR and visible camera imagery is the basis of our approach for SAR-MTI tracking problem
- This approach is used on processing the MTI hits on the ground plane SAR image
- The algorithm could exploit our analytical study of SAR geolocation based on radial-range and angular-Doppler shift information of MTI hits (that is discussed later)

Depiction of Association and Tracking

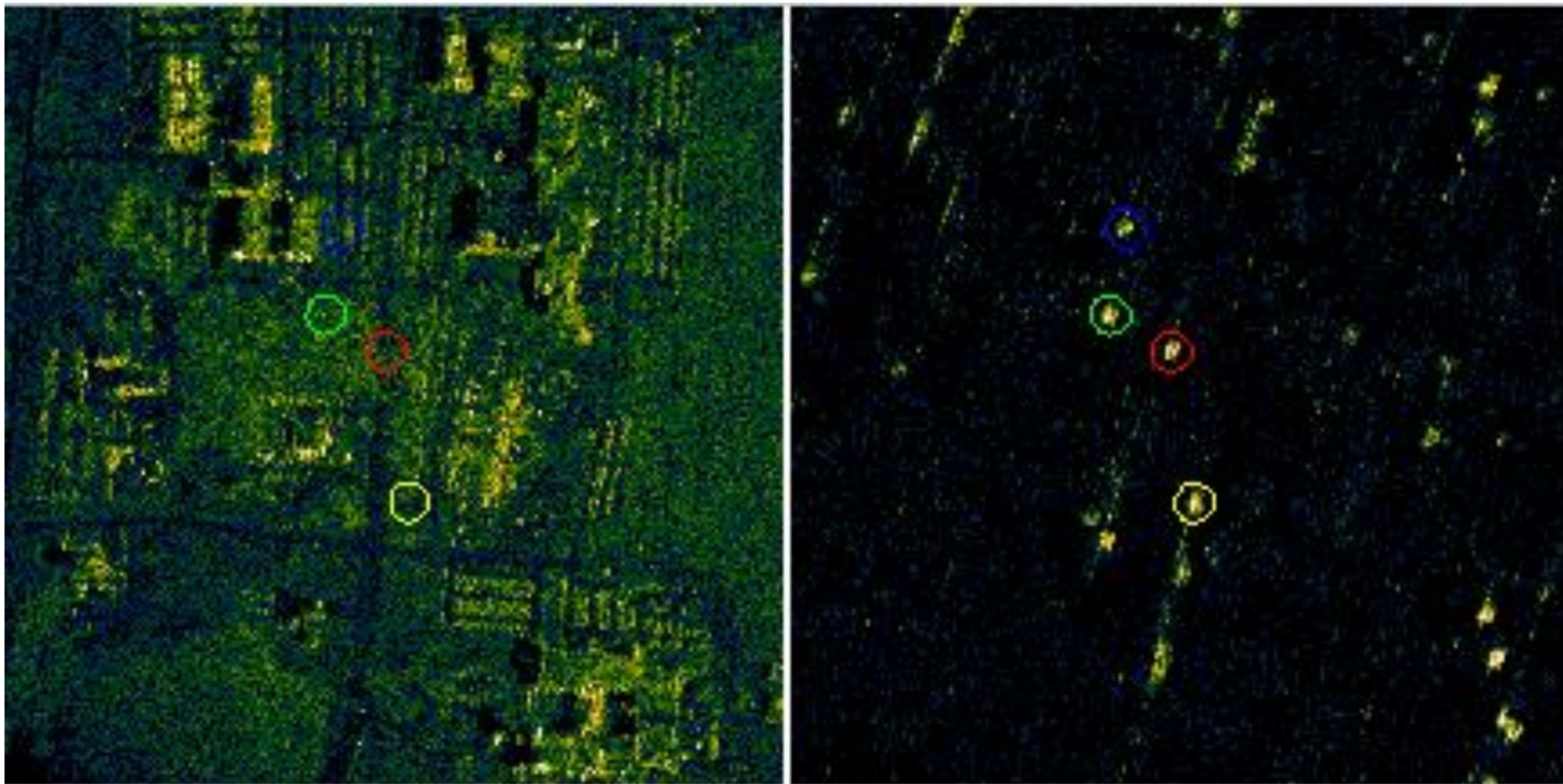
Algorithm



**MTI Tracks:
Coherent Single Pass
Dual Receivers
(DPCA-MTI)**



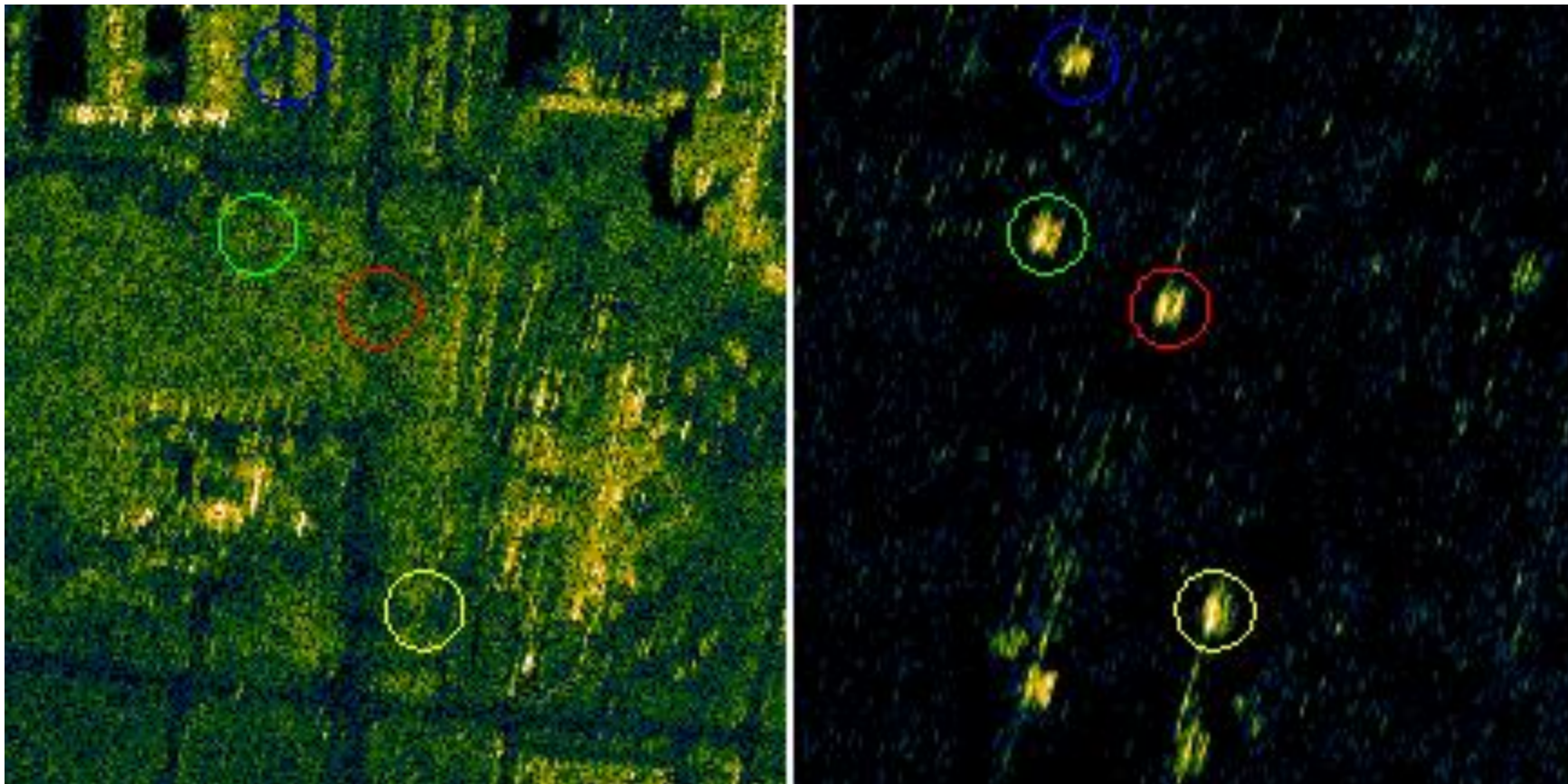
Tracks of Four Detected Moving Targets



Ground Plane

Public Release: Document Number 88 ABW-10-0809

Tracks of Four Detected Moving Targets



Ground Plane

Public Release: Document Number 88 ABW-10-0809

4.4 Ground Plane Geolocation

- Moving target coordinates at zero slow-time $\tau = 0$ of a subaperture:

$$\left(X_{\text{target}}^{(\ell)}, Y_{\text{target}}^{(\ell)}, Z_{\text{target}}^{(\ell)} \right)$$

- 3D velocity of moving target (is assumed to be a constant within a subaperture but may vary from one subaperture to another):

$$\left(v_{x\text{target}}^{(\ell)}, v_{y\text{target}}^{(\ell)}, v_{z\text{target}}^{(\ell)} \right)$$

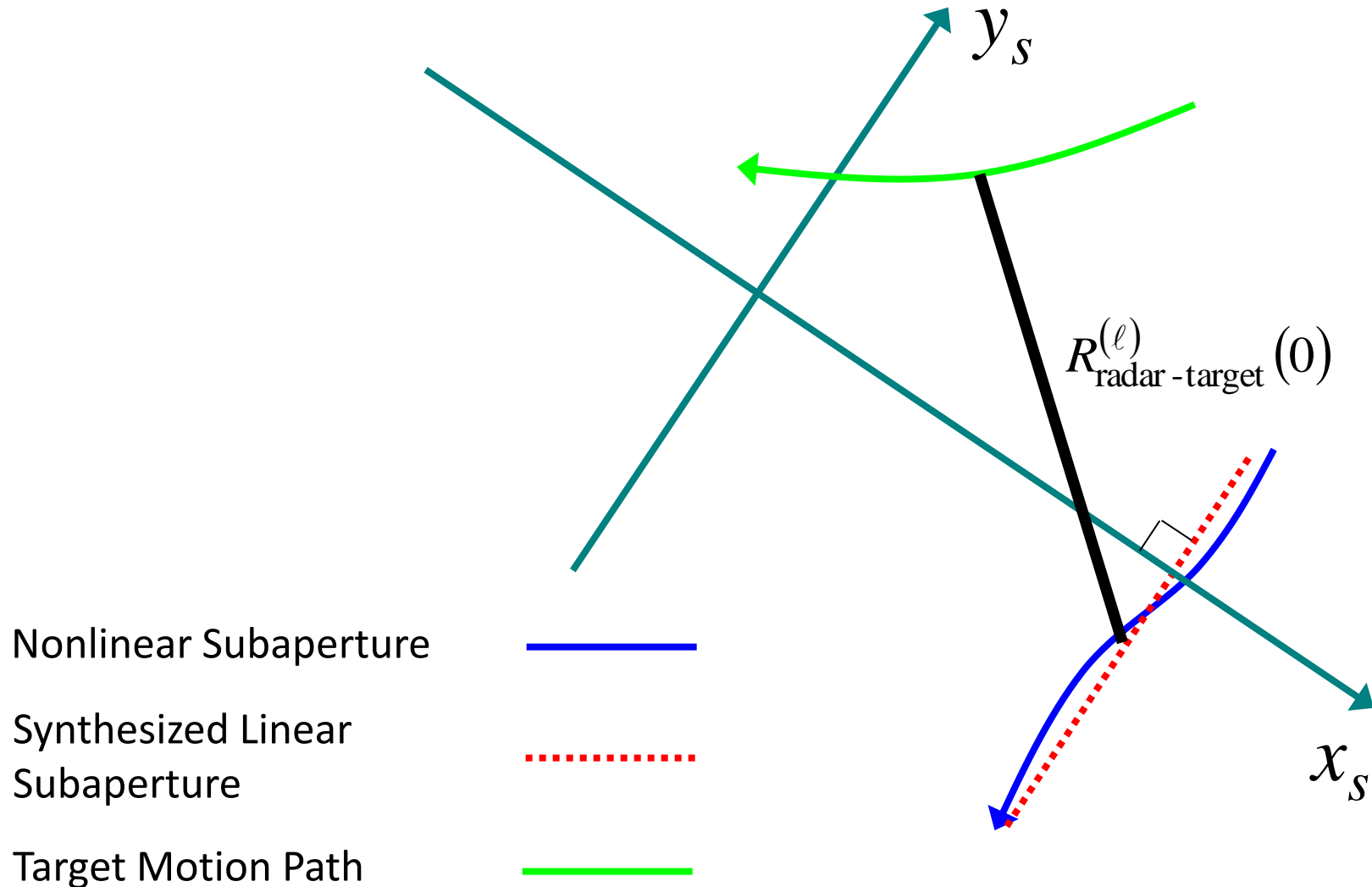
- Distance of moving target from radar (radial-range) as a function of slow-time:

$$R_{\text{radar-target}}^{(\ell)}(\tau) = \left[\begin{aligned} &\left(X_{\text{radar}}^{(\ell)} + v_{x\text{radar}}^{(\ell)} \tau - X_{\text{target}}^{(\ell)} - v_{x\text{target}}^{(\ell)} \tau \right)^2 + \\ &\left(Y_{\text{radar}}^{(\ell)} + v_{y\text{radar}}^{(\ell)} \tau - Y_{\text{target}}^{(\ell)} - v_{y\text{target}}^{(\ell)} \tau \right)^2 + \\ &\left(Z_{\text{radar}}^{(\ell)} + v_{z\text{radar}}^{(\ell)} \tau - Z_{\text{target}}^{(\ell)} - v_{z\text{target}}^{(\ell)} \tau \right)^2 \end{aligned} \right]^{1/2}$$

- Angular Doppler frequency of moving target as a function of slow-time:

$$\phi_{\text{radar-target}}^{(\ell)}(\tau)$$

Imaging System Geometry: Slant Plane



where

$$\sin \phi_{\text{radar-target}}^{(\ell)}(\tau) = \frac{\frac{d}{d\tau} R_{\text{radar-target}}^{(\ell)}(\tau)}{v_{\text{radar}}^{(\ell)}}$$

$$= \frac{\begin{bmatrix} \left(v_{x\text{radar}}^{(\ell)} - v_{x\text{target}}^{(\ell)} \right) \left(X_{\text{radar}}^{(\ell)} + v_{x\text{radar}}^{(\ell)} \tau - X_{\text{target}}^{(\ell)} - v_{x\text{target}}^{(\ell)} \tau \right) + \\ \left(v_{y\text{radar}}^{(\ell)} - v_{y\text{target}}^{(\ell)} \right) \left(Y_{\text{radar}}^{(\ell)} + v_{y\text{radar}}^{(\ell)} \tau - Y_{\text{target}}^{(\ell)} - v_{y\text{target}}^{(\ell)} \tau \right) + \\ \left(v_{z\text{radar}}^{(\ell)} - v_{z\text{target}}^{(\ell)} \right) \left(Z_{\text{radar}}^{(\ell)} + v_{z\text{radar}}^{(\ell)} \tau - Z_{\text{target}}^{(\ell)} - v_{z\text{target}}^{(\ell)} \tau \right) \end{bmatrix}}{v_{\text{radar}}^{(\ell)} R_{\text{radar-target}}^{(\ell)}(\tau)}$$

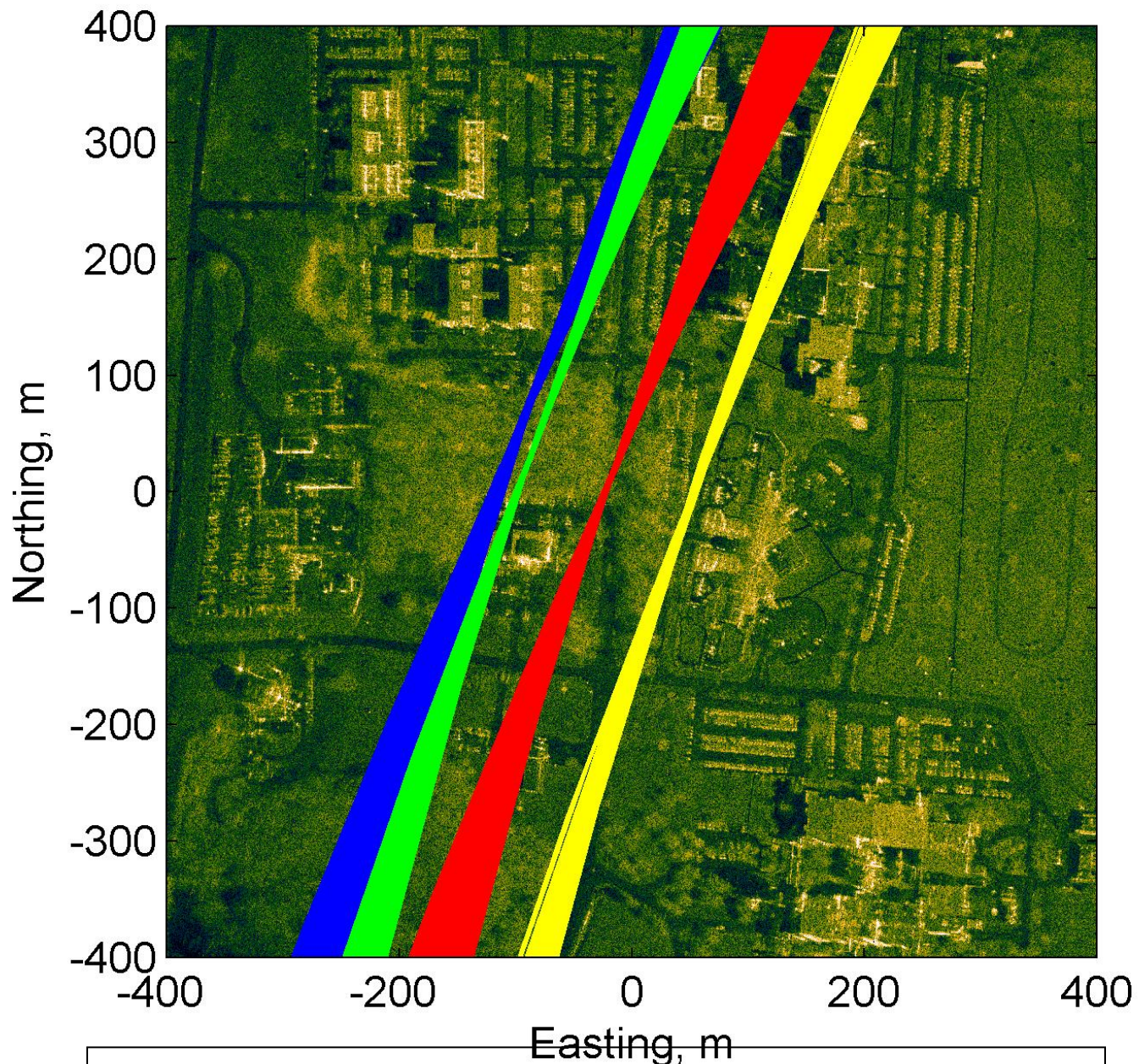
- For a subaperture image, moving target signature appears (centered) at

$$\left[\phi_{\text{radar-target}}^{(\ell)}(0), R_{\text{radar-target}}^{(\ell)}(0) \right]$$

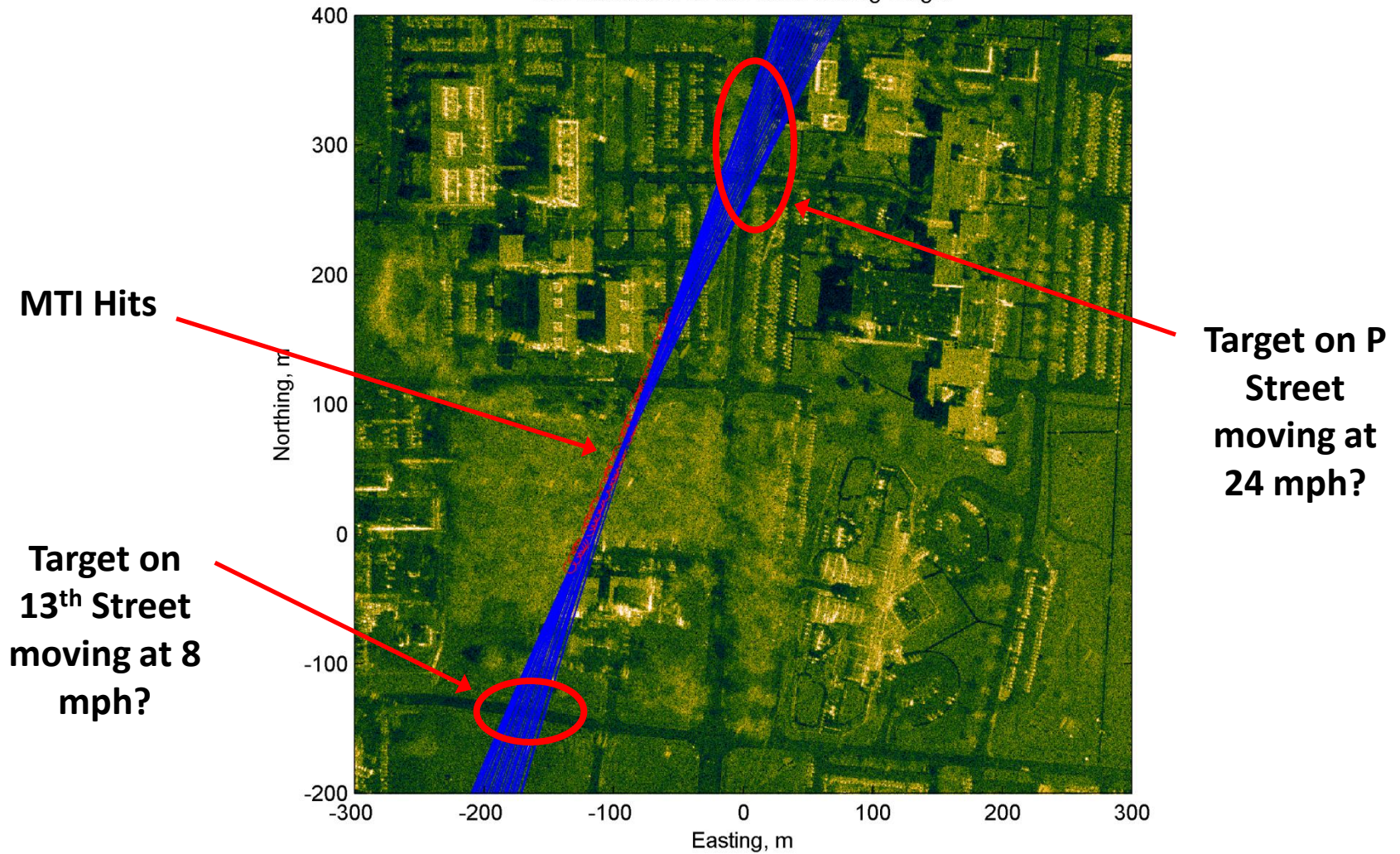
4.4.1 Geolocation Using Knowledge of Network of Roads

- Radial-ranges of a moving target for the subapertures could be mapped into the network of roads on the ground plane
- Operator/computer could determine which road is the logical/correct choice by:
 - a. Estimating target velocity on a road
 - b. Calculating subaperture angular Doppler values from the estimated velocity and other available radar/target parameters
 - c. Comparing calculated and actual angular Doppler data

UTM Recon and Motion Tracks: FP-128



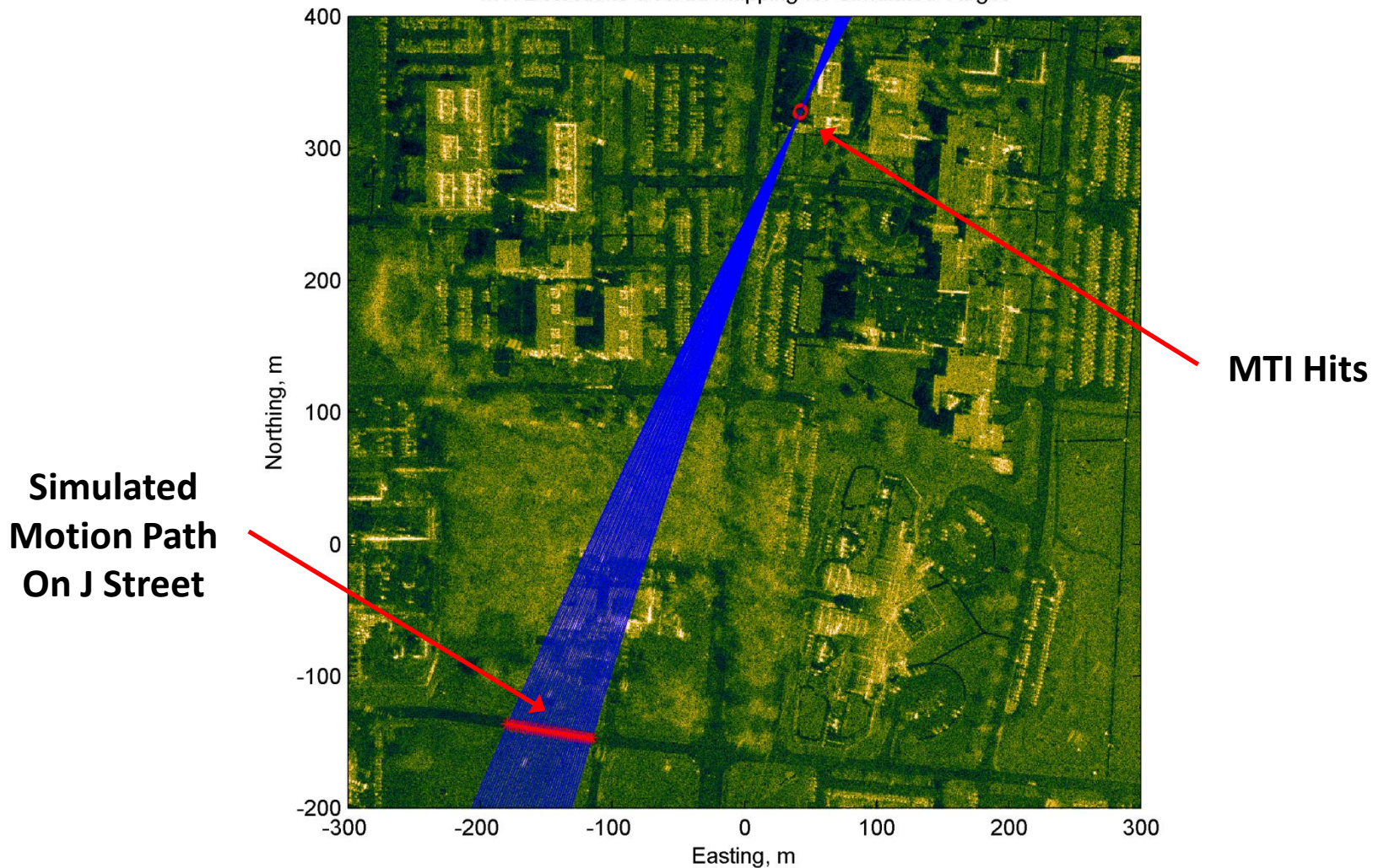
MTI Detections for an Acutal Moving Target



MTI detections for an actual moving target in subapertures 1-40 (red circles), and the lines of constant radial range for the moving target for each subaperture (blue lines)

MTI Results Validation and
Target Geolocation
via Measured SAR Data &
Simulation

MTI Detections & Road Mapping for Simulated Target

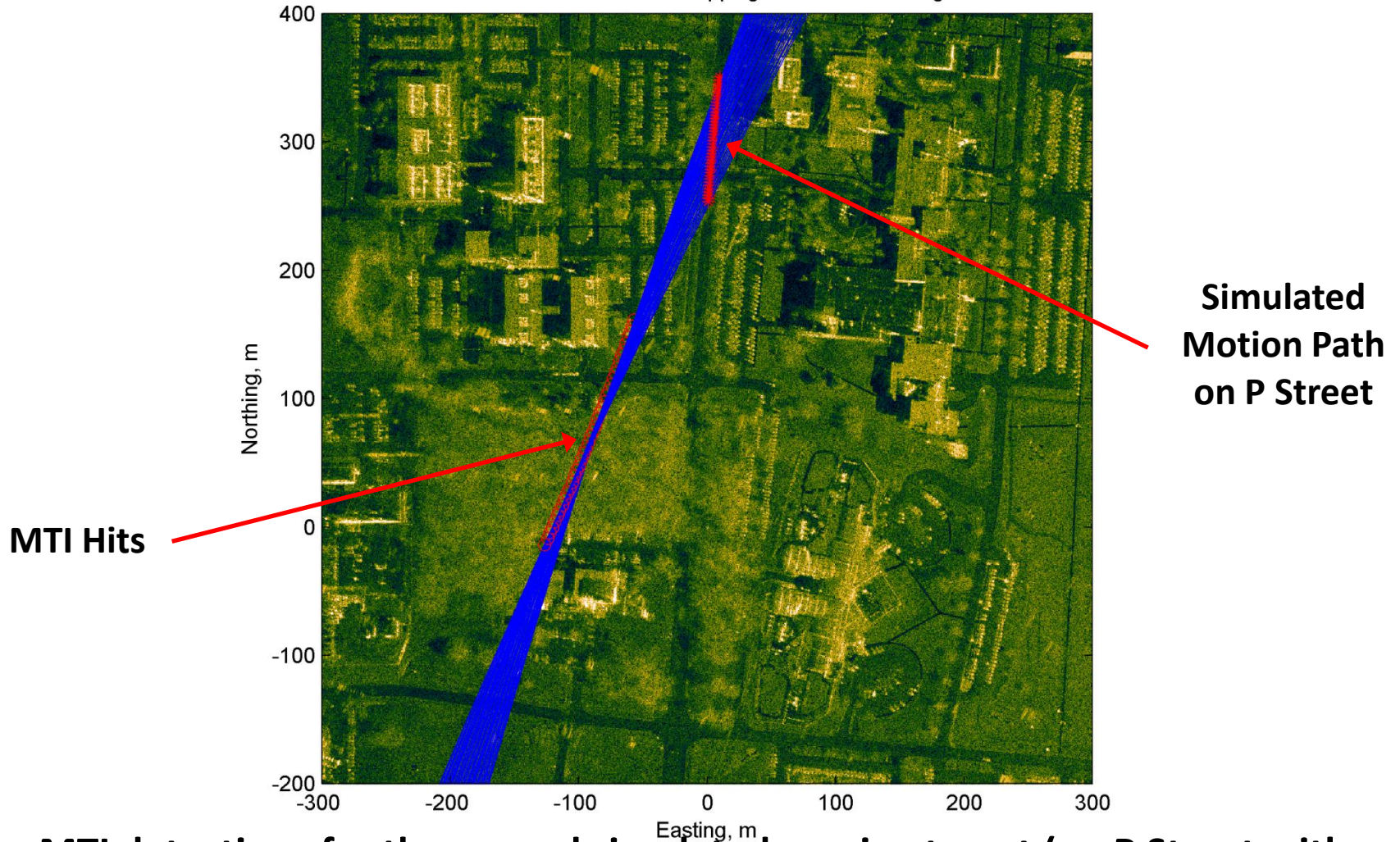


MTI detections for the first simulated moving target (on J Street with speed of 16 mph) in subapertures 1-40 (red circles), the lines of constant radial range for the moving target for each subaperture (blue lines), and the road mapping of the target on J Street (red stars)

**First Simulated
Moving Target
Tracks**

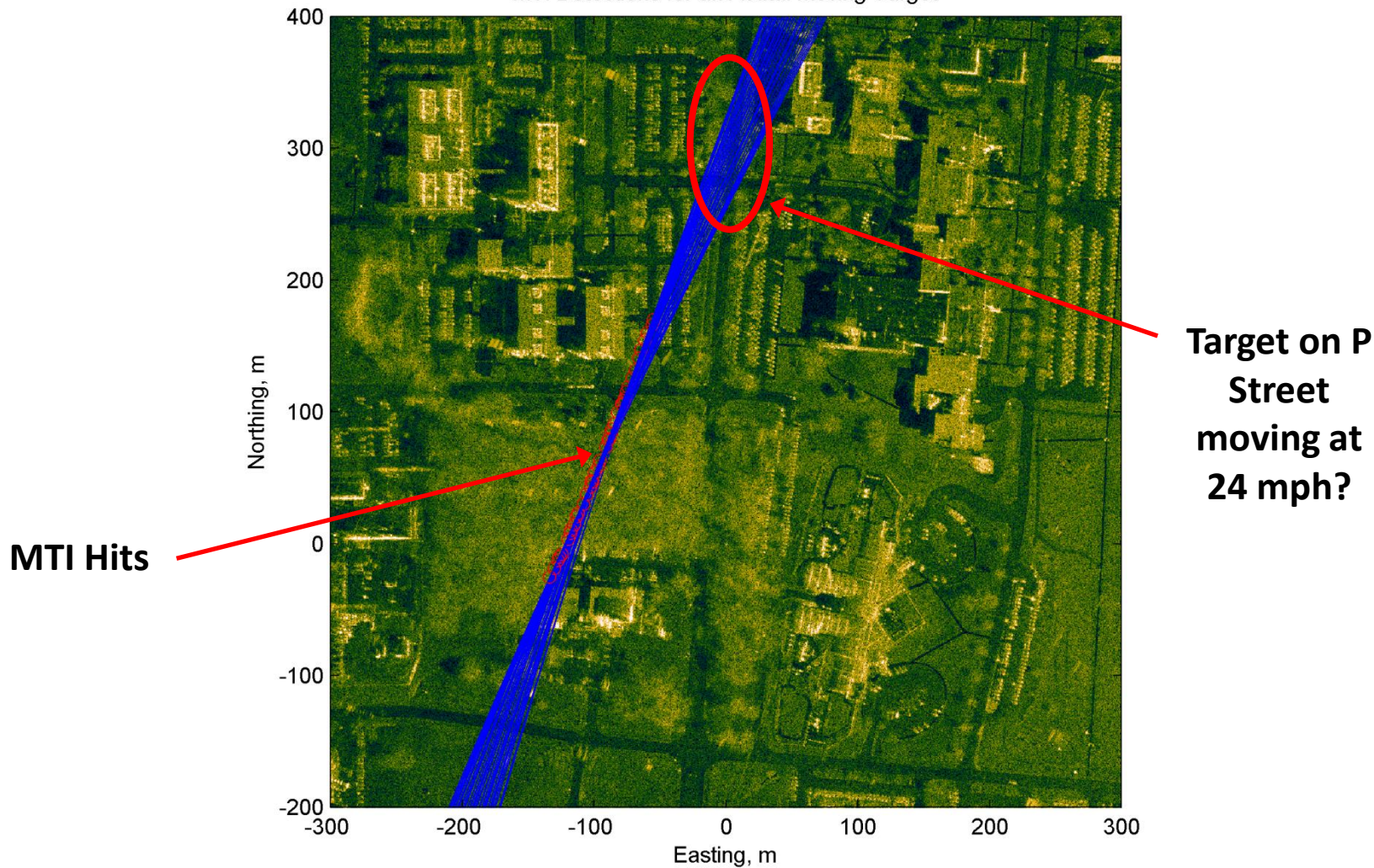


MTI Detections & Road Mapping for Simulated Target



MTI detections for the second simulated moving target (on P Street with speed of 24 mph) in subapertures 1-40 (red circles), the lines of constant radial range for the moving target for each subaperture (blue lines), and the road mapping of the target on P Street (red stars)

MTI Detections for an Acutal Moving Target



MTI detections for an actual moving target

Public Release: Document Number 88 ABW-10-0809

**Second
Simulated
Moving Target
Tracks**



- For the first simulated moving target on J Street, the MTI detections are closely located unlike the MTI detections of the actual moving target (even when the target speed is doubled to 16 mph)
- For the second moving target on P Street, its MTI hits are close to the MTI detections of the actual moving target

4.4.2 Geolocation Without Knowledge of Network of Roads

- For a subaperture image, moving target signature appears (centered) at radial-range and angular Doppler point:

$$\left[\phi_{\text{radar-target}}^{(\ell)}(0), R_{\text{radar-target}}^{(\ell)}(0) \right]$$

- Provided that moving target velocity is a constant for a set of subapertures, use nonlinear minimization to solve for moving target's six parameters (3D coordinates and velocity) from the knowledge of its multiple-subaperture radial-range and angular Doppler data

4.5 Application in Dismount Problem

- Due to relatively low speed of a dismount, one would not expect a Doppler shift in its signature
- Dismount signature in a SAR image would be fairly localized, and may not be detected via single pass noncoherent processing
- However, a dismount random/nonrandom motion would translate into phase differences in two channels of along-track monopulse (DPCA) SAR that could be detectable

5. Synthetic Aperture Radar Data Visualization on the Multi- touch screen Data table and iPod Touch

Topics to be Covered

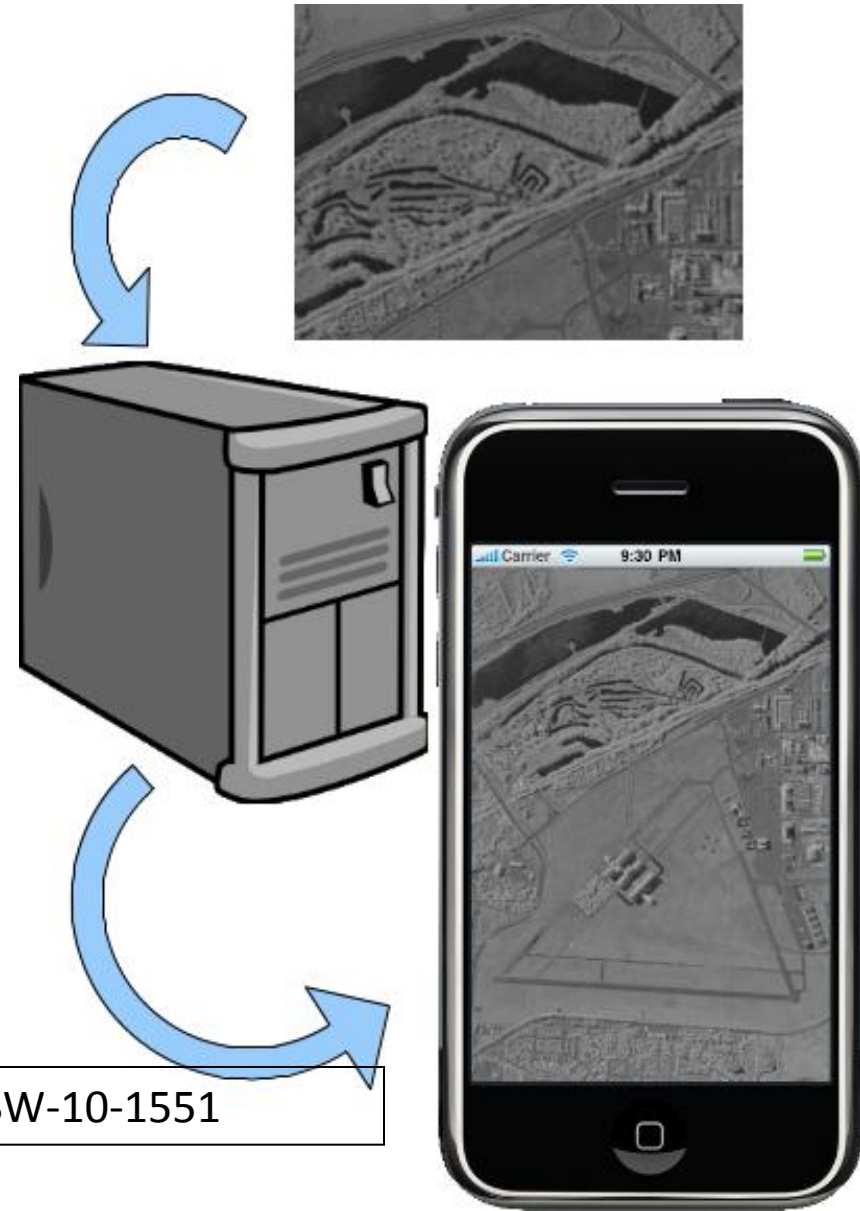
- ***Objective:*** Interface SAR images for real-time viewing and Forensic Analysis
- ***Hardware and Software:*** Multi-touch Screen, a HDTV, NASA Worldwind, WMS Server, iPod touch, and iPhone SDK

Objectives

- Provide a Google Earth-like interface for viewing real-time SAR data
- Very useful for users who need real-time information to make decisions
- Allow users to view data on mobile devices (iPhone/iPod touch/ iPad)
- Provides multiple levels of image detail

Key Components

- Video Synthetic Aperture Radar (SAR) will generate real-time movies at 1 frame per second
- SAR images are uploaded to a database which is accessed by a Web Map Service (WMS) server
- Data table/ iPhone application communicates with the WMS through URL requests to retrieve images and display them to the user



Data Table Demonstration



6. Summary

We Presented:

1. Advantage of *nonlinear* multi-channel, multi-polarization SAR data
2. Efficient/real-time Video SAR processing Algorithm
3. Examples of Video SAR, Coherent and non-coherent change detection
4. Multiple moving target detection and tracking
5. Multi-touch screen interface for SAR data visualization

What We Did Not Cover:

- Details ... tons of them ...